Perspective: Basic understanding of condensed phases of matter via packing models

S. Torquato

Citation: The Journal of Chemical Physics **149**, 020901 (2018); doi: 10.1063/1.5036657
View online: https://doi.org/10.1063/1.5036657
View Table of Contents: http://aip.scitation.org/toc/jcp/149/2
Published by the American Institute of Physics

Perspective: Basic understanding of condensed phases of matter via packing models

S. Torquato[a)]
Department of Chemistry, Department of Physics, Princeton Center for Theoretical Science, Princeton Institute for the Science and Technology of Materials, and Program in Applied and Computational Mathematics, Princeton University, Princeton, New Jersey 08544, USA

(Received 17 April 2018; accepted 14 June 2018; published online 10 July 2018)

Packing problems have been a source of fascination for millennia and their study has produced a rich literature that spans numerous disciplines. Investigations of hard-particle packing models have provided basic insights into the structure and bulk properties of condensed phases of matter, including low-temperature states (e.g., molecular and colloidal liquids, crystals, and glasses), multiphase heterogeneous media, granular media, and biological systems. The densest packings are of great interest in pure mathematics, including discrete geometry and number theory. This perspective reviews pertinent theoretical and computational literature concerning the equilibrium, metastable, and nonequilibrium packings of hard-particle packings in various Euclidean space dimensions. In the case of jammed packings, emphasis will be placed on the "geometric-structure" approach, which provides a powerful and unified means to quantitatively characterize individual packings via jamming categories and "order" maps. It incorporates extremal jammed states, including the densest packings, maximally random jammed states, and lowest-density jammed structures. Packings of identical spheres, spheres with a size distribution, and nonspherical particles are also surveyed. We close this review by identifying challenges and open questions for future research. *Published by AIP Publishing.*
https://doi.org/10.1063/1.5036657

I. INTRODUCTION

We will call a *packing* a large collection of nonoverlapping (i.e., hard) particles in either a finite-sized container or d-dimensional Euclidean space $\mathbb{R}^d$. Exclusion-volume effects that often arise in dense many-particle systems in physical and biological contexts are naturally captured by simple packing models. They have been studied to help understand the symmetry, structure, and physical properties of condensed matter phases, including liquids, glasses, and crystals, as well as the associated phase transitions.[1–18] Packings also serve as excellent models of the structure of multiphase heterogeneous materials,[19–22] colloids,[15,23,24] suspensions,[25,26] and granular media,[27,28] which enables predictions of their effective transport, mechanical, and electromagnetic properties.[20]

Packing phenomena are also ubiquitous in biological contexts and occur in systems across a wide spectrum of length scales. This includes DNA packing within the nucleus of a cell,[29] the "crowding" of macromolecules within living cells,[30] the packing of cells to form tissues,[20,31–33] the fascinating spiral patterns seen in plant shoots and flowers (phyllotaxis),[34,35] and the competitive settlement of territories.[20,36]

Understanding the symmetries and other mathematical properties of the densest sphere packings in various spaces and dimensions is a challenging area of long-standing interest in discrete geometry and number theory[37–39] as well as coding theory.[37,40,41] Packing problems are mathematically easy to pose, but they are notoriously difficult to solve rigorously. For example, in 1611, Kepler was asked the following question: What is the densest way to stack equal-sized cannon balls? His solution, known as "Kepler's conjecture," was the face-centered-cubic (fcc) arrangement (the way your green grocer stacks oranges). Gauss[42] proved that this is the densest Bravais lattice packing (defined below). Remarkably, nearly four centuries passed before Hales proved the general conjecture that there is no other sphere packing in three-dimensional (3D) Euclidean space whose density can exceed that of the fcc packing.[43] Even the proof that the densest packing of congruent (identical) circles in the plane is the triangular-lattice packing appeared only 80 years ago; see Refs. 37 and 39 for the history of this problem.

One objective of this perspective is to survey recent developments concerning the simplest but venerable packing model: identical frictionless spheres in the absence of gravity subject only to a nonoverlap constraint; i.e., the spheres do not interact for any nonoverlapping configuration. This "stripped-down" hard-sphere model can be viewed as the particle-system analog of the idealized Ising model for magnetic systems,[44] which is regarded as one of the pillars of statistical mechanics.[45–47] More complex packing models can include interactions that extend beyond hard-core distances, but our main concern here is the aforementioned classic version. This model enables one to uncover unifying principles that describe a broad range of phenomena, including the nature of equilibrium

[a)]torquato@princeton.edu

states of matter (e.g., liquids and crystals), metastable and nonequilibrium states of matter (e.g., supercooled liquids and structural glasses), and jamming phenomena.

Jammed sphere packings represent an important subset of hard-sphere configurations and have attracted great attention because they capture salient characteristics of crystals, glasses, granular media, and biological systems[27,32,44,48–53] and naturally arise in pure mathematical contexts.[37,54,55] Jammed packings are those in which each particle has a requisite number of contacting particles in order for the packing to achieve a certain level of mechanical stability. This review focuses on the so-called "geometric-structure" approach to jammed particle packings, which provides a powerful and unified means to quantitatively understand such many-particle systems. It incorporates not only the maximally dense packings and disordered jammed packings but also a myriad of other significant jammed states, including maximally random jammed (MRJ) states,[44,49] which can be regarded to be prototypical structural glasses, as well as the lowest-density jammed packings.[56]

Importantly, the simplified hard-sphere model embodies the primary structural attributes of dense many-particle systems in which steep repulsive interparticle interactions are dominant. For example, the densest sphere packings are intimately related to the (zero-temperature) ground states of such molecular systems[57] and high-pressure crystal phases. Indeed, the equilibrium hard-sphere model[12] also serves as a natural reference system in the thermodynamic perturbation theory of liquids characterized by steep isotropic repulsive interparticle interactions at short distances as well as short-range attractive interactions.[9,58] Moreover, the classic hard-sphere model provides a good description of certain classes of colloidal systems.[23,59–62] Note that the hard-core constraint does not uniquely specify the hard-sphere model; there are an infinite number of nonequilibrium hard-sphere ensembles, some of which will be surveyed.

We will also review work that describes generalizations of this simplified hard-sphere model to include its natural extension to packings of hard spheres with a size distribution. This topic has relevance to understanding dispersions of technological importance (e.g., solid propellant combustion,[63] flow in packed beds,[64] and sintering of powders[65]), packings of biological cells, and phase behavior of various molecular systems. For example, the densest packings of hard-sphere mixtures are intimately related to high-pressure phases of compounds for a range of temperatures.[66,67] Another natural extension of the hard-sphere model that will be surveyed is hard *nonspherical* particles in two and three dimensions. Asphericity in particle shape is capable of capturing the salient features of phases of molecular systems with anisotropic pair interactions (e.g., liquid crystals) and is also a more realistic characteristic of real granular media. In addition, we will review the aspects of dense sphere packings in high-dimensional Euclidean spaces, which provide useful physical insights and are relevant to error-correcting codes and information theory.[37,40]

We begin this perspective by introducing relevant definitions and background (Sec. II). This is followed by a survey of work on equilibrium, metastable, and nonequilibrium packings of identical spheres and polydisperse spheres in one, two, and three dimensions (Sec. III). The geometric structure approach to jammed and unjammed packings, including their classification via order maps, is emphasized. Subsequently, the corresponding results for sphere packings in high Euclidean and non-Euclidean space dimensions (Sec. IV) and packings of nonspherical particles in low-dimensional Euclidean spaces (Sec. V) are reviewed. Finally, we describe some challenges and open questions for future research (Sec. VI).

II. DEFINITIONS AND BACKGROUND

A *packing* P is a collection of nonoverlapping solid objects or particles of general shape in d-dimensional Euclidean space $\mathbb{R}^d$. Packings can be defined in other spaces (e.g., hyperbolic spaces and compact spaces, such as the surface of a d-dimensional sphere), but our primary focus in this review is $\mathbb{R}^d$. A *saturated* packing is the one in which there is no space available to add another particle of the same kind to the packing. The *packing fraction* ϕ is the fraction of space $\mathbb{R}^d$ covered by the particles.

A d-dimensional particle is *centrally symmetric* if it has a center C that bisects every chord through C connecting any two boundary points of the particle; i.e., the center is a point of inversion symmetry. Examples of centrally symmetric particles in $\mathbb{R}^d$ include spheres, ellipsoids, and superballs (defined in Sec. V). A triangle and a tetrahedron are examples of non-centrally symmetric 2D and 3D particles, respectively. A d-dimensional centrally symmetric particle for $d \geq 2$ is said to possess d equivalent principal axes (orthogonal directions) associated with the moment of inertia tensor if these directions are two-fold rotational symmetry axes. Whereas a d-dimensional superball has d equivalent directions, a d-dimensional ellipsoid generally does not. The reader is referred to Ref. 44 for further discussion concerning particle symmetries.

A *lattice* Λ in $\mathbb{R}^d$ is a subgroup consisting of the integer linear combinations of vectors that constitute a basis for $\mathbb{R}^d$. In the physical sciences, this is referred to as a *Bravais* lattice. The term "lattice" will refer here to a Bravais lattice only. Every lattice has a dual (or reciprocal) lattice Λ^* in which the lattice sites are specified by the dual (reciprocal) lattice vectors.[37] A *lattice packing* P_L is the one in which the centroids of the nonoverlapping identical particles are located at the points of Λ, and all particles have a common orientation. The set of lattice packings is a subset of all possible packings in $\mathbb{R}^d$. In a lattice packing, the space $\mathbb{R}^d$ can be geometrically divided into identical regions F called *fundamental cells*, each of which has volume $\mathrm{Vol}(F)$ and contains the centroid of just one particle of volume v_1. Thus, the lattice packing fraction is

$$\phi = \frac{v_1}{\mathrm{Vol}(F)}. \tag{1}$$

Common d-dimensional lattices include the *hypercubic* $\mathbb{Z}^d$, *checkerboard* D_d, and *root* A_d lattices; see Ref. 37. Following Conway and Sloane,[37] we say two lattices are *equivalent* or *similar* if one becomes identical to the other possibly by

a rotation, reflection, and change of scale, for which we use the symbol ≡. The A_d and D_d lattices are d-dimensional generalizations of the face-centered-cubic (fcc) lattice defined by $A_3 \equiv D_3$; however, for $d \geq 4$, they are no longer equivalent. In two dimensions, $A_2 \equiv A_2^*$ is the triangular lattice. In three dimensions, $A_3^* \equiv D_3^*$ is the body-centered-cubic (bcc) lattice. In four dimensions, the checkerboard lattice and its dual are equivalent, i.e., $D_4 \equiv D_4^*$. The hypercubic lattice $\mathbb{Z}^d \equiv \mathbb{Z}_*^d$ and its dual lattice are equivalent for all d.

A *periodic* packing of congruent particles is obtained by placing a fixed configuration of N particles (where $N \geq 1$) with *arbitrary orientations* subject to the nonoverlapping condition in one fundamental cell of a lattice Λ, which is then periodically replicated. Thus, the packing is still periodic under translations by Λ, but the N particles can occur anywhere in the chosen fundamental cell subject to the overall nonoverlap condition. The packing fraction of a periodic packing is given by

$$\phi = \frac{N v_1}{\mathrm{Vol}(F)} = \rho v_1, \tag{2}$$

where $\rho = N/\mathrm{Vol}(F)$ is the number density, i.e., the number of particles per unit volume.

For simplicity, consider a packing of N identical d-dimensional spheres of diameter D centered at the positions $\mathbf{r}^N \equiv \{\mathbf{r}_1, \mathbf{r}_2, \ldots, \mathbf{r}_N\}$ in a region of volume V in d-dimensional Euclidean space $\mathbb{R}^d$. Ultimately, we will pass to the *thermodynamic limit*, i.e., $N \to \infty$, $V \to \infty$ such that the *number density* $\rho = N/V$ is a fixed positive constant and its corresponding packing fraction is given by

$$\phi = \rho v_1(D/2), \tag{3}$$

where

$$v_1(R) = \frac{\pi^{d/2}}{\Gamma(1 + d/2)} R^d \tag{4}$$

is the volume of a d-dimensional sphere of radius R and $\Gamma(x)$ is the gamma function. For an individual sphere, the *kissing* or *contact* number Z is the number of spheres that may simultaneously touch this sphere. In a sphere packing, the *mean* kissing or contact number per particle, $\overline{Z}$, is the average of Z over all spheres. For lattice packings, $Z = \overline{Z}$. For statistically homogeneous sphere packings in $\mathbb{R}^d$, the quantity $\rho^n g_n(\mathbf{r}^n)$ is proportional to the probability density associated with simultaneously finding n sphere centers at locations $\mathbf{r}^n \equiv \{\mathbf{r}_1, \mathbf{r}_2, \ldots, \mathbf{r}_n\}$ in $\mathbb{R}^d$; see Ref. 12 and the references therein. With this convention, each *n-particle correlation function* g_n approaches unity when all particles become widely separated from one another for any system without long-range order. Statistical homogeneity implies that g_n is translationally invariant and therefore only depends on the relative displacements of the positions with respect to some arbitrarily chosen origin of the system, i.e., $g_n = g_n(\mathbf{r}_{12}, \mathbf{r}_{13}, \ldots, \mathbf{r}_{1n})$, where $\mathbf{r}_{ij} = \mathbf{r}_j - \mathbf{r}_i$.

The *pair correlation* function $g_2(\mathbf{r})$ is of basic interest in this review. If the system is also rotationally invariant (statistically isotropic), then g_2 depends on the radial distance $r \equiv |\mathbf{r}|$ only, i.e., $g_2(\mathbf{r}) = g_2(r)$. The *total correlation* function is defined by $h(\mathbf{r}) \equiv g_2(\mathbf{r}) - 1$. Importantly, we focus in this review on *disordered* packings in which $h(\mathbf{r})$ decays to zero for large $|\mathbf{r}|$ sufficiently rapidly so that its volume integral over all space exists.[68]

As usual, we define the non-negative *structure factor* $S(\mathbf{k})$ for a statistically homogeneous packing as

$$S(\mathbf{k}) = 1 + \rho \tilde{h}(\mathbf{k}), \tag{5}$$

where $\tilde{h}(\mathbf{k})$ is the Fourier transform of $h(\mathbf{r})$ and $\mathbf{k}$ is the wave vector. The non-negativity of $S(\mathbf{k})$ for all $\mathbf{k}$ follows physically from the fact that it is proportional to the intensity of the scattering of incident radiation on a many-particle system.[12] The structure factor $S(\mathbf{k})$ provides a measure of the density fluctuations in particle configurations at a particular wave vector $\mathbf{k}$. For any point configuration in which the minimal pair distance is some positive number, such as a sphere packing, $g_2(\mathbf{r} = \mathbf{0}) = 0$, and $h(\mathbf{r} = \mathbf{0}) = -1$, the structure factor obeys the following sum rule:[69]

$$\frac{1}{(2\pi)^d} \int_{\mathbb{R}^d} [S(\mathbf{k}) - 1]\, d\mathbf{k} = -\rho. \tag{6}$$

For a single-component system in thermal equilibrium at number density ρ and absolute temperature T, the structure factor at the origin is directly related to the isothermal compressibility κ_T via the relation[12]

$$\rho k_B T \kappa_T = S(0), \tag{7}$$

where k_B is the Boltzmann constant.

It is well known from Fourier transform theory that if a real-space radial function $f(r)$ in $\mathbb{R}^d$ decreases sufficiently rapidly to zero for large r such that all of its even moments exist, then its Fourier transform $\tilde{f}(k)$, where $k \equiv |\mathbf{k}|$ is a wavenumber, is an even and analytic function at $k = 0$. Hence, $S(k)$, defined by (5), has an expansion about $k = 0$ in any space dimension d of the general form

$$S(k) = S_0 + S_2 k^2 + \mathcal{O}(k^4), \tag{8}$$

where S_0 and S_2 are the d-dependent constants, defined by

$$S_0 = 1 + d\rho s_1(1) \int_0^\infty r^{d-1} h(r) dr \geq 0 \tag{9}$$

and

$$S_2 = -\frac{\rho s_1(1)}{2d} \int_0^\infty r^{d+1} h(r) dr, \tag{10}$$

where

$$s_1(R) = \frac{d\, \pi^{d/2} R^{d-1}}{\Gamma(d/2 + 1)} \tag{11}$$

is the surface area of the d-dimensional sphere of radius R. This behavior is to be contrasted with that of maximally random jammed sphere packings,[49] which possess a structure factor that is nonanalytic at $k = 0$ (Ref. 70), as discussed in greater detail in Sec. III E.

A hyperuniform[71] point configuration in $\mathbb{R}^d$ is the one in which the structure factor $S(\mathbf{k})$ tends to zero as the wavenumber tends to zero, i.e.,

$$\lim_{|\mathbf{k}| \to 0} S(\mathbf{k}) = 0, \tag{12}$$

implying that single scattering of incident radiation at infinite wavelengths is completely suppressed. Equivalently, a hyperuniform system is the one in which the number variance

$\sigma_N^2(R) \equiv \langle N(R)^2\rangle - \langle N(R)\rangle^2$ of particles within a spherical observation window of radius R grows more slowly than the window volume, i.e., R^d, in the large-R limit. Point configurations of this class include perfect crystals, many perfect quasicrystals, and special disordered many-particle systems.[71–73] Note that the structure-factor definition (5) and the hyperuniformity requirement (12) dictate that the following *sum rule* involving $h(\mathbf{r})$ that a hyperuniform point process must obey

$$\rho \int_{\mathbb{R}^d} h(\mathbf{r}) d\mathbf{r} = -1. \tag{13}$$

This sum rule implies that $h(\mathbf{r})$ must exhibit negative correlations, i.e., *anticorrelations*, for some values of $\mathbf{r}$.

The hyperuniformity concept was generalized to incorporate two-phase heterogeneous media (e.g., composites, porous media, and dispersions).[72,74] Here the phase volume fraction fluctuates within a spherical window of radius R and hence can be characterized by the volume-fraction variance $\sigma_V^2(R)$. For typical disordered two-phase media, the variance $\sigma_V^2(R)$ for large R goes to zero like R^{-d}. However, for hyperuniform disordered two-phase media, $\sigma_V^2(R)$ goes to zero asymptotically more rapidly than the inverse of the window volume, i.e., faster than R^{-d}, which is equivalent to the following condition on the *spectral density* $\tilde{\chi}_V(\mathbf{k})$:[74]

$$\lim_{|\mathbf{k}|\to 0} \tilde{\chi}_V(\mathbf{k}) = 0. \tag{14}$$

The spectral density is proportional to the scattered intensity associated with "mass" (volume) content of the phases.[75]

III. SPHERE PACKINGS IN LOW DIMENSIONS

The classical statistical mechanics of hard-sphere systems has generated a huge collection of scientific publications, dating back at least to Boltzmann;[76] see also Refs. 12 and 77–79. Here we focus on packings of frictionless congruent spheres of diameter D in one, two, and three dimensions in the absence of gravity.

It is important to observe that the impenetrability constraint alone of this idealized hard-sphere model does not uniquely specify the statistical ensemble. Hard-sphere systems can be in thermal equilibrium (as discussed in Sec. III A) or derived from one of an infinite number of nonequilibrium ensembles[20] (see Sec. III B for examples).

A. Equilibrium and metastable phase behavior

The phase behavior of hard spheres provides powerful insights into the nature of liquid, crystal, and metastable states as well as the associated phase transitions in molecular and colloidal systems. It is well known that the pressure p of a stable thermodynamic phase in $\mathbb{R}^d$ at packing fraction ϕ and temperature T is simply related to the contact value of the pair correlation function, $g_2(D^+)$,[20]

$$\frac{p}{\rho k_B T} = 1 + 2^{d-1}\phi g_2(D^+). \tag{15}$$

Away from jammed states, it has been proved that the mean nearest-neighbor distance between spheres, λ, is bounded from the above by the pressure,[48] namely, $\lambda \le 1 + 1/[2d(p/(\rho k_B T) - 1]$.

Figure 1 schematically shows the 3D phase behavior in the ϕ–p plane. At sufficiently low densities, an infinitesimally slow compression of the system at constant temperature defines a thermodynamically stable liquid branch for packing fractions up to the "freezing" point ($\phi \approx 0.49$). Increasing the density beyond the freezing point putatively results in an entropy-driven first-order phase transition[77,80] to a crystal branch that begins at the melting point ($\phi \approx 0.55$). While there is no rigorous proof that such a first-order freezing transition occurs in three dimensions, there is overwhelming simulational evidence for its existence, beginning with the pioneering work of Alder and Wainwright.[77] Slow compression of the system along the crystal branch must end at one of the optimal (maximally dense) sphere packings with $\phi = \pi/\sqrt{18} = 0.740\,48\ldots$, each of which is a jammed packing in which each particle contacts 12 others (see Sec. III D). This equilibrium state has an infinite pressure and is putatively entropically favored by the fcc packing.[81] It is noteworthy that the melting mechanism of the corresponding equilibrium 2D hard-disk system has been poorly understood over the last fifty years. A relatively recent Monte Carlo study capable of thermalizing sufficiently large systems (as required) reveals that melting in such systems proceeds in two steps: a first-order liquid-hexatic phase transition and then a continuous hexatic-solid phase transition.[18]

Importantly, compressing a hard-sphere liquid rapidly, under the constraint that significant crystal nucleation is suppressed, can produce a range of metastable branches whose density end points are disordered "jammed" packings,[16,20,82]

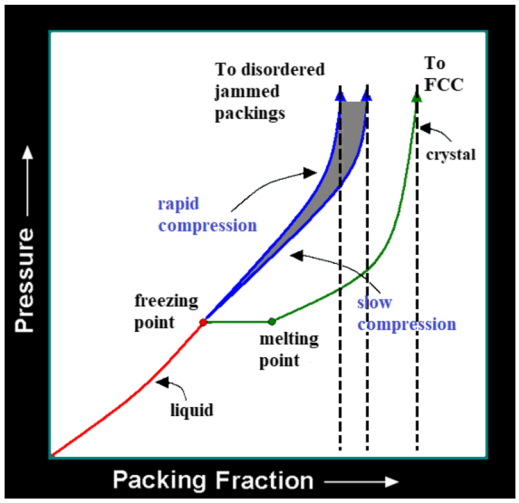

FIG. 1. The isothermal phase behavior of the 3D hard-sphere model in the pressure-packing fraction plane, as adapted from Ref. 44. Three different isothermal densification paths by which a hard-sphere liquid may jam are shown. An infinitesimal compression rate of the liquid traces out the thermodynamic equilibrium path (shown in green), including a discontinuity resulting from the first-order freezing transition to a crystal branch that ends at a maximally dense infinite-pressure jammed state. Rapid compressions of the liquid while suppressing some degree of local order (blue curves) can avoid crystal nucleation (on short time scales) and produce a range of amorphous metastable extensions of the liquid branch that jam only at their density maxima. Adapted with permission from S. Torquato and F. H. Stillinger, Rev. Mod. Phys. **82**, 2633 (2010). Copyright 2010 American Physical Society.

which can be regarded to be glasses. A rapid compression leads to a lower random jammed density than that for a slow compression. The most rapid compression ending in mechanically stable packing is presumably the maximally random jammed (MRJ) state[49] with $\phi \approx 0.64$. Accurate approximate formulas for the pressure along such metastable extensions up to the jamming points have been obtained.[20,83] This ideal amorphous state is described in greater detail in Sec. III E. Note that rapid compression of a hard-sphere system is analogous to supercooling of a molecular liquid.

Pair statistics are exactly known only in the case of 1D "hard-rod" systems.[84] For $d \geq 2$, approximate formulas for $g_2(r)$ are known along liquid branches.[12] Approximate closures of the Ornstein-Zernike integral equation linking the direct correlation function $c(r)$ to the total correlation function $h(r)$,[85] such as the Percus-Yevick (PY) and hypernetted chain schemes,[2,7,12,86] provide reasonably accurate estimates of $g_2(r)$ for hard-sphere liquids. Because $g_2(r)$ decays to unity exponentially fast for liquid states, we can conclude that it must have a corresponding structure factor $S(k)$ that is an even function and analytic at $k = 0$; see Eq. (8). Also, since the leading-order term S_0 must be positive because the isothermal compressibility is positive [cf. (7)], classic hard-sphere liquids are not hyperuniform. Figure 2 shows $g_2(r)$ and the corresponding structure factor $S(k)$ in three dimensions at $\phi = 0.35$ as obtained from the PY approximation. Note that the Percus-Yevick approximations for 2D and 3D systems do not exhibit structural precursors to the respective freezing transitions, as manifested by "shoulders" in the second peak of $g_2(r)$ observed in computer simulations.[17]

It is noteworthy that one can create "stealthy" hyperuniform hard-sphere packings[87] by decorating points derived from stealthy equilibrium configurations[88] with nonoverlapping spheres.

B. Nonequilibrium disordered packings

Here we briefly discuss three different nonequilibrium sphere packings: random sequential addition (RSA), "ghost" random sequential addition, and random close packing (RCP).

1. Random sequential addition

Perhaps one of the most well-known nonequilibrium packing models is the random sequential addition (RSA) packing procedure, which is a time-dependent process that generates disordered sphere packings in $\mathbb{R}^d$; see Refs. 89–97. The RSA packing process in the first three space dimensions has been used to model a variety of different condensed phases, including protein adsorption,[92] polymer oxidation,[98] particles in cell membranes,[91] and ion implantation in semiconductors.[99]

In its simplest rendition, an RSA sphere packing is produced by randomly, irreversibly, and sequentially placing nonoverlapping objects into a large volume in $\mathbb{R}^d$ that at some initial time is empty of spheres. If an attempt to add a sphere at some time t results in an overlap with an existing sphere in the packing, the attempt is rejected and further attempts are made until it can be added without overlapping existing spheres. One can stop the addition process at any finite time t, obtaining an RSA configuration with a time-dependent packing fraction $\phi(t)$, but this value cannot exceed the maximal *saturation* packing fraction $\phi_s = \phi(\infty)$ that occurs in the infinite-time and thermodynamic limits. Even at the saturation state, the spheres are never in contact and hence are not *jammed* in the sense described in Sec. III C; moreover, the pair correlation function $g_2(r)$ decays to unity for large r super-exponentially fast.[100] The latter property implies that the structure factor $S(k)$ of RSA packings in $\mathbb{R}^d$ must be an even and analytic function at $k = 0$,[96] as indicated in Eq. (8). It is notable that saturated RSA packings are not hyperuniform for any finite space dimension.[96,97]

In the one-dimensional case, also known as the "car-parking" problem, the saturation packing fraction was obtained analytically: $\phi_s = 0.747\,597\,920\,2\ldots$.[89] However, for $d \geq 2$, ϕ_s in the thermodynamic limit has only been estimated via numerical simulations. The most precise numerical study to date[97] has yielded $\phi_s = 0.547\,073\,5 \pm 0.000\,002\,8$ for $d = 2$ and $\phi_s = 0.384\,130\,7 \pm 0.000\,002\,1$ for $d = 3$. Estimates of ϕ_s in higher dimensions are discussed in Sec. IV. RSA packings have also been examined for spheres with a size distribution[101] and other particle shapes, including squares,[92,102,103] rectangles,[104] ellipses,[103] superdisks,[105] and polygons[106,107] in $\mathbb{R}^2$ and spheroids,[108] spherocylinders,[103] and cubes[109,110] in $\mathbb{R}^3$.

2. "Ghost" random sequential addition

There is a generalization of the aforementioned standard RSA process, which can be viewed as a "thinning" process of a Poisson distribution of sphere and is parameterized by the positive constant κ that lies in the closed interval [0, 1]; see Ref. 111. When $\kappa = 0$, one recovers the standard RSA process, and when $\kappa = 1$, one obtains the "ghost"

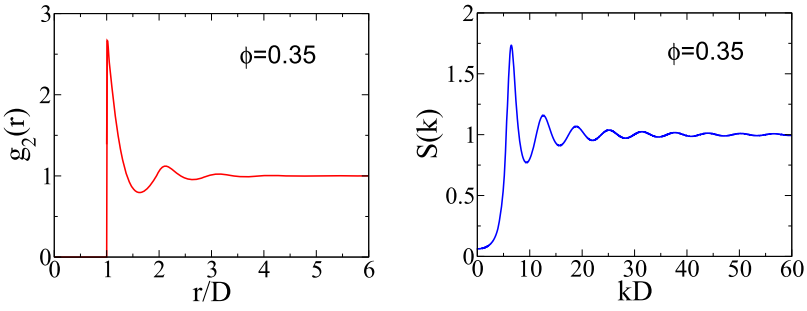

FIG. 2. Pair statistics for an equilibrium hard-sphere fluid in three dimensions at $\phi = 0.35$ as obtained from the PY approximation.[2,12] Left panel: Pair correlation function $g_2(r)$ versus r/D, where D is the sphere diameter. Right panel: The corresponding structure factor $S(k)$ as a function of the dimensionless wavenumber kD, which clearly shows nonhyperuniformity.

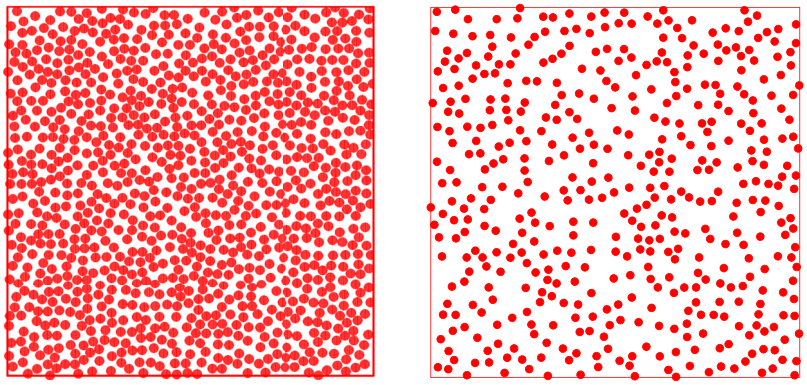

FIG. 3. Examples of two nonequilibrium packing models in two dimensions under periodic boundary conditions. Left panel: A configuration of the standard RSA packing at saturation with $\phi_s \approx 0.5$. Right panel: A configuration of a ghost RSA packing at a packing fraction ϕ very near its maximal value of 0.25. Note that the packing is clearly unsaturated (as defined in Sec. II) and there are no contacting particles.

random sequential addition (RSA) process that enables one to obtain exactly not only the time-dependent packing fractions but all of the n-particle correlation functions g_n for any n and d. The reader is referred to Ref. 111 for details about the general model.

In the ghost RSA process, one attempts to place spheres into an initially empty region of space randomly, irreversibly, and sequentially. However, here one keeps track of any rejected sphere, which is called a "ghost" sphere. No additional spheres can be added whenever they overlap an existing sphere or a ghost sphere. The packing fraction at time t for spheres of unit diameter is given by $\phi(t) = [1 - \exp(-v_1(1)t)]/2^d$, where $v_1(R)$ is the volume of sphere of radius R. Thus, we see that as $t \to +\infty$, $\phi = 2^{-d}$, which is appreciably smaller than the RSA saturation packing fraction ϕ_s in low dimensions; see Fig. 3 for 2D examples. Nonetheless, it is notable that the ghost RSA process is the only hard-sphere packing model that is exactly solvable for any dimension d and all realizable densities, which has implications for high-dimensional packings, as discussed in Sec. IV.

3. Random close packing

The "random close packing" (RCP) notion was pioneered by Bernal[3–5] to model the structure of liquids and has been one of the more persistent themes with a venerable history.[112–119] Two decades ago, the prevailing notion of the RCP state was that it is the *maximum* density that a large random collection of congruent (identical) spheres can attain and that this density is a well-defined quantity. This traditional view has been summarized as follows: "Ball bearings and similar objects have been shaken, settled in oil, stuck with paint, kneaded inside rubber balloons–and all with no better result than (a packing fraction of) . . .0.636"; see Ref. 113.

Torquato, Truskett, and Debenedetti[49] have argued that this RCP-state concept is actually ill-defined because "randomness" and "closed-packed" were never defined and, even if they were, are at odds with one another. Using the Lubachevsky-Stillinger (LS)[120] molecular-dynamics growth algorithm to generate jammed packings, it was shown[49] that fastest particle growth rates generated the most disordered sphere packings with $\phi \approx 0.64$, but that by slowing the growth rates larger packing fractions could be continuously achieved up to the densest value $\phi_{\max} = 0.740\,48\ldots$ such that the degree of order increased monotonically with ϕ. These results demonstrated that one can increase the packing fraction by an arbitrarily small amount at the expense of correspondingly small increases in order, and thus, the notion of RCP is ill-defined as the highest possible density that a random sphere packing can attain. To remedy these flaws, Torquato, Truskett, and Debenedetti[49] replaced the notion of "close packing" with "jamming" categories (defined precisely in Sec. III C) and introduced the notion of an "order metric" to quantify the degree of order (or disorder) of a single packing configuration. This led them to supplant the concept of RCP with the maximally random jammed (MRJ) state, which is defined, roughly speaking, to be that jammed state with a minimal value of an order metric (see Sec. III C 4 for details). This work pointed the way toward a quantitative means of characterizing all packings, namely, the geometric-structure approach.

We note that whereas the LS packing protocol with a fast growth rate typically leads to disordered jammed states in three dimensions, it invariably produces highly crystalline "collectively" jammed packings in two dimensions. Figure 4 vividly illustrates the differences between the textures produced in three and in two dimensions (see Sec. III B for further remarks).

C. Geometric-structure approach to jammed packings

A "jammed" packing is the one in which each particle is in contact with its nearest neighbors such that the mechanical stability of a specific type is conferred to the packing, as detailed below. Two conceptual approaches for their study have emerged. One is the "ensemble" approach,[3,5,27,50–52,122–129] which for a given packing protocol aims to understand typical configurations and their frequency of occurrence. The other more recent one is the "geometric-structure" approach,[49,56,121,130–134] which emphasizes quantitative characterization of single-packing configurations without regard to their occurrence frequency in the protocol used to produce them. Here we focus on the latter approach, which enables one to enumerate and classify packings with a diversity of order/disorder and packing fractions, including extremal packings, such as the densest sphere packing and MRJ packings.

1. Jamming categories

Three broad and mathematically precise "jamming" categories of sphere packings can be distinguished depending on

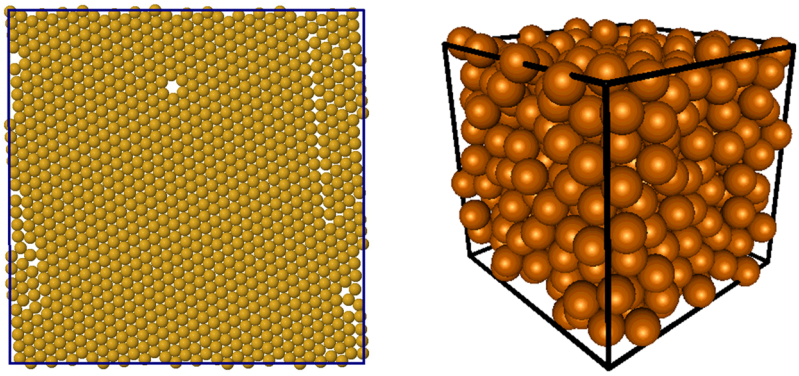

FIG. 4. Typical protocols, used to generate disordered sphere packings in three dimensions, produce highly crystalline packings in two dimensions. Left panel: A highly ordered collectively jammed configuration (Sec. III C 1) of 1000 disks with $\phi \approx 0.88$ produced using the Lubachevsky-Stillinger (LS) algorithm[120] with a fast expansion rate.[121] Right panel: A 3D MRJ-like configuration of 500 spheres with $\phi \approx 0.64$ produced using the LS algorithm with a fast expansion rate.[49]

the nature of their mechanical stability.[71,130] In the order of increasing stringency (stability), for a finite sphere packing, these are the following:

1. *Local jamming*: Each particle in the packing is locally trapped by its neighbors (at least $d + 1$ contacting particles, not all in the same hemisphere); i.e., it cannot be translated, while fixing the positions of all other particles.
2. *Collective jamming:* Any locally jammed configuration is collectively jammed if no subset of particles can be simultaneously displaced so that its members move out of contact with one another and with the remainder set.
3. *Strict jamming:* Any collectively jammed configuration that disallows all uniform volume-nonincreasing strains of the system boundary.

These hierarchical jamming categories are closely related to the concepts of "rigid" and "stable" packings found in the mathematics literature[135] and imply that there can be no "rattlers" (i.e., movable but caged particles) in the packing. The jamming category of a given packing depends on the boundary conditions employed; see Refs. 44 and 130 for specific examples. Rigorous and efficient linear-programming (LP) algorithms have been devised to assess whether a particular sphere packing is locally, collectively, or strictly jammed.[121,136] These jamming categories can now be ascertained in real-system experiments by applying the LP tests to configurational coordinates of a packing determined via a variety of imaging techniques, including tomography,[137] confocal microscopy,[138] and magnetic resonance imaging.[139]

2. Polytope picture and pressure in jamming limit

A packing of N hard spheres of diameter D in a jammed framework in $\mathbb{R}^d$ is specified by an Nd-dimensional configurational position vector $\mathbf{R} = \mathbf{r}^N \equiv \{\mathbf{r}_1, \ldots, \mathbf{r}_N\}$. *Isostatic* jammed packings possess the minimal number of contacts for a jamming category and boundary conditions.[140] The relative differences between isostatic collective and strict jammed packings diminish as N becomes large, and since the number of degrees of freedom is essentially equal to Nd, an isostatic packing has a *mean contact number per particle*, $\overline{Z}$, equal to $2d$ in the large-N limit. Packings having more and fewer contacts than the isostatic ones are *hyperstatic* and *hypostatic*, respectively. Sphere packings that are hypostatic cannot be collectively or strictly jammed.[134]

Consider decreasing the density slightly in a sphere packing that is at least collectively jammed by reducing the particle diameter by ΔD so that the packing fraction is lowered to $\phi = \phi_J(1-\delta)^d$, where $\delta = \Delta D/D \ll 1$ is called the *jamming gap* or distance to jamming. There is a sufficiently small δ that does not destroy the jamming confinement property. For fixed N and sufficiently small δ, it can be shown asymptotically, through first order in δ, that the set of displacements accessible to the packing approaches a convex *limiting polytope* (a high-dimensional polyhedron) $\mathcal{P}$.[8,79] This polytope $\mathcal{P}$ is determined from the linearized impenetrability equations[121,136] and is necessarily bounded for a jammed configuration.

Now consider adding thermal kinetic energy to a nearly jammed sphere packing in the *absence of rattlers*. While the system will not be globally ergodic over the full system configuration space and thus not in thermodynamic equilibrium, one can still define a macroscopic pressure p for the trapped but locally ergodic system by considering time averages as the system executes a tightly confined motion around the *particular* jammed configuration $\mathbf{R_J}$. The probability distribution $P_f(f)$ of the *time-averaged* interparticle forces f has been rigorously linked to the contact value $r = D$ of the pair correlation function $g_2(r)$.[140] Moreover, the available (free) configuration volume scales with the jamming gap δ such that the reduced pressure is asymptotically given by the free-volume equation of state,[8,79,140]

$$\frac{p}{\rho k_B T} \sim \frac{1}{\delta} = \frac{d}{1-\phi/\phi_J}, \tag{16}$$

where T is the absolute temperature and ρ is the number density. Relation (16) is remarkable, since it enables one to determine accurately the true jamming density of a given packing, even if the actual jamming point has not quite yet been reached, just by measuring the pressure and extrapolating to $p = +\infty$. This free-volume form has been used to estimate the equation of state along "metastable" extensions of the hard-sphere fluid up to the infinite-pressure endpoint, assumed to be disordered jammed states (see Fig. 1 and Sec. III A).[20,83]

Kamien and Liu[141] assumed the same free-volume form to fit data for the pressure of "metastable" hard-sphere states.

3. Hard-particle jamming algorithms

For many years, the Lubachevsky-Stillinger (LS) algorithm[120] has served as the premier numerical scheme to generate a wide spectrum of dense jammed hard-sphere packings with variable disorder in both two and three dimensions.[49,131,142] This is an event-driven or a collision-driven molecular-dynamics algorithm: an initial configuration of spheres of a given size within a periodic cell are given initial random velocities and the motion of the spheres are followed as they collide elastically and also grow uniformly until the spheres can no longer expand. The final density is generally inversely related to the particle growth rate. This algorithm has been generalized by Donev, Torquato, and Stillinger[143,144] to generate jammed packings of smoothly shaped nonspherical particles, including ellipsoids,[134,144] superdisks,[145] and superballs.[146] Event-driven packing protocols with growing particles, however, do not guarantee jamming of the final packing configuration, since jamming is not explicitly incorporated as a termination criterion.

The task of generating dense packings of particles of general shape within an adaptive periodic fundamental cell has been posed by Torquato and Jiao[147,148] as an optimization problem called the *adaptive-shrinking cell* (ASC) scheme. The negative of the packing fraction, $-\phi$ (which can be viewed as an "energy"), is to be minimized subject to constraints. The design variables are the centroids and orientations of the particles as well as the shape and size of the deformable periodic fundamental cell, which is completely specified by a strain tensor. For nonspherical particles, the nonoverlap constraints are generally highly nonlinear and so the ASC optimization problem is solved using a Monte Carlo procedure.[147,148] The so-called Torquato-Jiao (TJ) sphere-packing algorithm[149] is a sequential linear-programming (SLP) solution of the ASC optimization problem for the special case of packings of spheres with a size distribution for which linearization of the design variables is *exact*. The deterministic SLP solution in principle always leads to strictly jammed packings up to a high numerical tolerance with a wider range of densities and degree of disorder than packings produced by the LS algorithm. From an initial configuration, the TJ algorithm leads to a mechanically stable local "energy" minimum (local density maximum), which in principle is the inherent structure associated with the starting initial many-particle configuration; see Fig. 5. A broad range of inherent structures can be obtained across space dimensions, including locally maximally dense and mechanically stable packings, such as MRJ states,[149–152] disordered hyperstatic packings,[153] and the globally maximally dense inherent structures,[149,154–157] with very small computational cost, provided that the system sizes are not too large.

It is notable that the TJ algorithm creates disordered jammed sphere packings that are closer to the ideal MRJ state than previous algorithms.[150] It was shown that the rattler concentration of these packings converges toward 1.5% in the infinite-system limit, which is markedly lower than previous estimates for the MRJ state using the LS protocol (with about 3% rattlers).

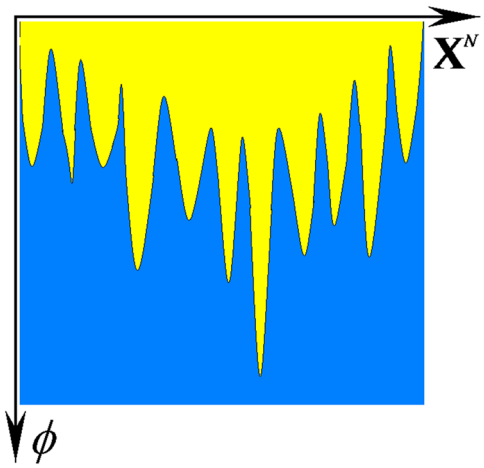

FIG. 5. A schematic diagram of inherent structures (local density maxima) for sphere packings of N spheres, as taken from Ref. 149. The horizontal axis labeled $\mathbf{X}^N$ stands for the entire set of centroid positions and $-\phi$ ("energy") decreases downward. The jagged curve is the boundary between the accessible configurations (yellow) and inaccessible ones (blue). The deepest point of the accessible configurations corresponds to the maximal density packings of hard spheres. Reprinted with permission from S. Torquato and Y. Jiao, Phys. Rev. E **82**, 061302 (2010). Copyright 2010 American Physical Society.

4. Order metrics

The enumeration and classification of both ordered and disordered sphere packings is an outstanding problem. Since the difficulty of the complete enumeration of packing configurations rises exponentially with the number of particles, it is desirable to devise a small set of intensive parameters that can characterize packings well. One obvious property of a sphere packing is the packing fraction ϕ. Another important characteristic of a packing is some measure of its "randomness" or degree of disorder. Devising such measures is a highly nontrivial challenge, but even the tentative solutions that have been put forth during the last two decades have been fruitfully applied to characterize not only sphere packings[49,71,131,142] but also simple liquids,[16,142,158,159] glasses,[142,160] water,[161,162] disordered ground states,[88] random media,[163] and biological systems.[32]

It is quite reasonable to consider "entropic" measures to characterize the randomness of packings. However, as pointed out by Kansal *et al.*,[131] a substantial hurdle to overcome in implementing such an order metric is the necessity to generate all possible jammed states or, at least, a representative sample of such states in an unbiased fashion using a "universal" protocol in the large-system limit, each of which is an intractable problem. Even if such a universal protocol could be developed, however, the issue of what weights to assign the resulting configurations remains. Moreover, there are other basic problems with the use of entropic measures as order metrics, as we will discuss in Sec. III E, including its significance for certain 2D hard-disk packings.

We know that a many-body system of N particles is completely characterized statistically by its N-body probability density function $P(\mathbf{R}; t)$ that is associated with finding the N-particle system with configuration $\mathbf{R}$ at some time t. Such

complete information is virtually never available for large N and, in practice, one must settle for reduced information, such as a scalar order metric ψ. Any order metric ψ conventionally possesses the following three properties: (1) it is a well-defined scalar function of a configuration $\mathbf{R}$; (2) it is subject typically to the normalization $0 \le \psi \le 1$; and (3) for any two configurations $\mathbf{R}_A$ and $\mathbf{R}_B$, $\psi(\mathbf{R}_A) > \psi(\mathbf{R}_B)$ implies that configuration $\mathbf{R}_A$ is to be considered as more ordered than configuration $\mathbf{R}_B$. The set of order metrics that one selects is unavoidably subjective, given that there appears to be no single universally applicable scalar metric capable of describing order across all length scales. However, one can construct order metrics that lead to consistent results, as will be discussed below.

Many relevant order metrics have been devised. While a comprehensive discussion of this topic is beyond the scope of this article, it is useful here to note some order metrics that have been identified, including bond-orientational order metrics in two[164] and three dimensions,[165] translational order metrics,[49,88,142] and hyperuniformity order metrics.[71,72] These specific order metrics have both strengths and weaknesses. This raises the question of what are the characteristics of a good order metric? It has been suggested that a good scalar order metric should have the following additional properties:[44,131] (1) sensitivity to any type of ordering without bias toward any reference system; (2) ability to reflect the hierarchy of ordering between prototypical systems given by common physical intuition (e.g., perfect crystals with high symmetry should be highly ordered, followed by quasicrystals, correlated disordered packings without long-range order, and finally spatially uncorrelated or Poisson distributed particles); (3) incorporation of both the variety of local coordination patterns as well as the spatial distribution of such patterns should be included; and (4) the capacity to detect translational and orientational order at any length scale. Moreover, any useful set of order metrics should consistently produce results that are positively correlated with one another.[20,49] The development of improved order metrics deserves continued research attention.

Order metrics and maps have been fruitfully extended to characterize the degree of structural order in condensed phases in which the constituent particles (jammed or not) possess both attractive and repulsive interactions. This includes the determination of the order maps of models of simple liquids, glasses, and crystals with isotropic interactions,[16,142,158,159] models of water,[161,162] disordered ground states of long-ranged isotropic pair potentials,[88] and models of amorphous polymers.[166]

D. Order maps and extremal packings

The geometric-structure classification naturally emphasizes that there is a great diversity in the types of attainable packings with varying magnitudes of overall order, packing fraction ϕ, and mean contact number per particle, $\overline{Z}$, among many other intensive parameters. Any attainable hard-sphere configuration, jammed or not, can be mapped to a point in this multidimensional parameter space that we call an *order map*. The use of "order maps" in combination with the mathematically precise "jamming categories" enables one to view and characterize individual packings, including the densest sphere packing (e.g., Kepler's conjecture in 3D) and MRJ packings as extremal states in the order map for a given jamming category. Indeed, this picture encompasses not only these special jammed states but also an uncountably infinite number of other packings, some of which have only recently been identified as physically significant, e.g., the jamming-threshold states[56] (least dense jammed packings) as well as states between these and MRJ.

The simplest order map is the one that maps any hard-sphere configuration to a point in the ϕ–ψ plane. This two-parameter description is but a very small subset of the relevant parameters that are necessary to fully characterize a configuration, but it nonetheless enables one to draw important conclusions. Figure 6 shows such an order map that delineates the set of strictly jammed packings[49,56,121,131] from non-jammed packings in three dimensions. The boundaries of the jammed region delineate extremal structures (see Fig. 7). The densest sphere packings,[43] which lie along the locus B-B' with $\phi_{\max} = \pi/\sqrt{18} \approx 0.74$, are strictly jammed.[121,130] Point B corresponds to the face-centered-cubic (fcc) packing; i.e., it is the *most ordered* and *symmetric* densest packing, implying that their shear moduli are infinitely large.[132] The most disordered subset of the stacking variants of the fcc packing is denoted by point B'. In two dimensions, the strictly jammed triangular lattice is the unique densest packing[167] and so the line B-B' in $\mathbb{R}^3$ collapses to a single point B in $\mathbb{R}^2$.

The least dense strictly jammed packings are conjectured to be the "tunneled crystals" in $\mathbb{R}^3$ with $\phi_{\min} = 2\phi_{\max}/3 = 0.493\,65\ldots$, corresponding to the locus of points $A - A'$.[56] These infinitely degenerate sparse structures were analytically determined by appropriate stackings of planar "honeycomb" layers of spheres. These constitute a set of zero measure among the possible packings with the same density and thus are virtually impossible to discover using packing

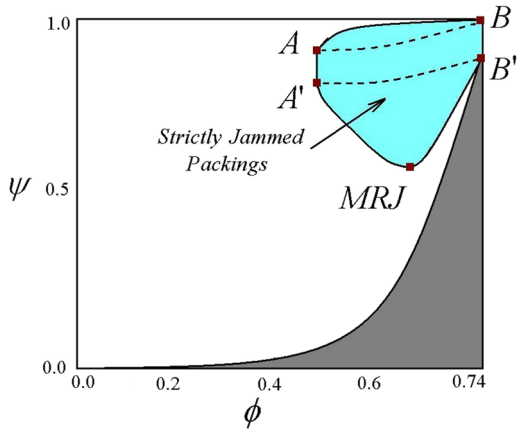

FIG. 6. Schematic *order map* of sphere packings in $\mathbb{R}^3$ in the density-order (ϕ–ψ) plane. White and blue regions contain the attainable packings, blue regions represent the jammed subspaces, and dark shaded regions contain no packings. The boundaries of the jammed region delineate *extremal* structures. The locus of points A-A' correspond to the lowest-density jammed packings. The locus of points B-B' correspond to the densest jammed packings. Points MRJ represent the maximally random jammed states, i.e., the most disordered states subject to the jamming constraint.

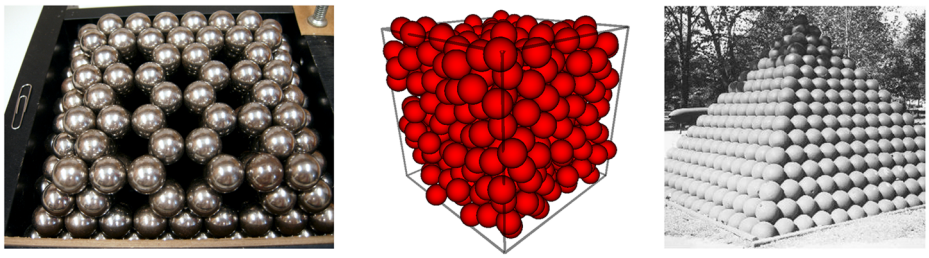

FIG. 7. Three different extremal strictly jammed packings in $\mathbb{R}^3$ identified in Fig. 6, as taken from Ref. 44. Left panel: A tunneled crystal with $Z = 7$ corresponding to point A in Fig. 6. Middle panel: MRJ packing with $Z = 6$ (isostatic) corresponding to point MRJ in Fig. 6. Right panel: fcc packing with $Z = 12$ corresponding to point B in Fig. 6. Reprinted with permission from S. Torquato and F. H. Stillinger, Rev. Mod. Phys. **82**, 2633 (2010). Copyright 2010 American Physical Society.

algorithms, illustrating the importance of analyzing individual packings, regardless of their frequency of occurrence in the space of jammed configurations, as advocated by the geometric-structure approach. The tunneled crystals are subsets of the densest packings but are permeated with infinitely long chains of particle vacancies.[56] Every sphere in a tunneled crystal contacts 7 immediate neighbors. Interestingly, the tunneled crystals exist at the edge of mechanical stability, since removal of any one sphere from the interior would cause the entire packing to collapse. The tunneled crystals are magnetically frustrated structures and Burnell and Sondhi[168] showed that their underlying topologies greatly simplify the determination of their antiferromagnetic properties. In $\mathbb{R}^2$, the "reinforced" kagomé packing with exactly four contacts per particle (isostatic value) is evidently the lowest density strictly jammed packing[121] with $\phi_{\min} = \sqrt{3}\pi/8 = 0.680\,17\ldots$ and so the line A-A' in $\mathbb{R}^3$ collapses to a single point A in $\mathbb{R}^2$.

E. Maximally random jammed states

Among all strictly jammed sphere packings in $\mathbb{R}^d$, the one that exhibits maximal disorder (minimizes some given order metric ψ) is of special interest. This is called the maximally random jammed (MRJ) state;[49] see Fig. 6. The MRJ state is automatically compromised by passing either to the maximal packing fraction (fcc and its stacking variants) or the minimal possible density for strict jamming (tunneled crystals), thereby causing any reasonable order metric to rise on either side. A variety of sensible order metrics produce a 3D MRJ state with a packing fraction $\phi_{\mathrm{MRJ}} \approx 0.64$ (see Ref. 131), close to the traditionally advocated density of the RCP state, and with an isostatic mean contact number $\overline{Z} = 6$ (see Ref. 140). This consistency among the different order metrics speaks to their utility, even if a perfect order metric has not yet been identified. However, the density of the MRJ state is not sufficient to fully specify it. It is possible to have a rather ordered strictly jammed packing at this very same density,[131] as indicated in Fig. 6. The MRJ state refers to a single packing that is maximally disordered subject to the strict jamming constraint, regardless of its probability of occurrence in some packing protocol. Thus, the MRJ state is conceptually and quantitatively different from random close packed (RCP) packings,[3–5] which, more recently, have been suggested to be the most probable jammed configurations within an ensemble.[51] The differences between these states are even starker in two dimensions; e.g., MRJ packings of identical circular disks in $\mathbb{R}^2$ have been shown to be dramatically different from their RCP counterparts, including their respective densities, average contact numbers, and degree of order,[151] as detailed below.

The MRJ state under the strict-jamming constraint is a prototypical glass[56] in that it is maximally disordered (according to a variety of order metrics) without any long-range order (Bragg peaks) and perfectly rigid (i.e., the elastic moduli are unbounded[44,132]). Its pair correlation function can be decomposed into a Dirac-delta-function contribution from particle contacts and a continuous-function contribution $g_2^{cont}(r)$,

$$g_2(r) = \frac{Z}{\rho s_1(D)}\delta(r - D) + g_2^{cont}(r), \tag{17}$$

where $s_1(R)$ is given by (11), $\delta(r)$ is a radial Dirac delta function, and $Z = 2d$. The corresponding structure factor in the long-wavenumber limit is

$$S(k) \sim 1 + \frac{2Z}{s_1(1)}\left(\frac{2\pi}{kD}\right)^{\frac{d-1}{2}} \cos[kD - (d-1)\pi/4] \quad (k \to \infty). \tag{18}$$

For $d = 3$, $g_2^{cont}(r)$ possesses the well-known feature of a split second peak,[169] with a prominent discontinuity at twice the sphere diameter, as shown in Fig. 8. Interestingly, an integrable power-law divergence ($1/r^{\alpha}$ with $\alpha \approx 0.4$) exists for near contacts.[70,140] Moreover, an MRJ packing in $\mathbb{R}^d$ has a structure factor $S(\mathbf{k})$ that tends to zero linearly in $|\mathbf{k}|$ (within numerical error) in the limit $|\mathbf{k}| \to 0$ and hence is hyperuniform (see Fig. 8), belonging to the same class as Fermi-sphere point processes[170] and superfluid helium in its ground state.[171,172] This *nonanalytic* behavior at $|\mathbf{k}| = 0$ implies that MRJ packings are characterized by negative "quasi-long-range" (QLR) pair correlations in which the total correlation function $h(\mathbf{r})$ decays to zero asymptotically like $-1/|\mathbf{r}|^{d+1}$; see Refs. 69, 70, 152, and 173–175. The QLR hyperuniform behavior distinguishes the MRJ state strongly from that of the equilibrium hard-sphere fluid,[176] which possesses a structure factor that is analytic at $\mathbf{k} = \mathbf{0}$ [cf. (8)], and thus, its $h(r)$ decays to zero exponentially fast for large r; see Ref. 44. Interestingly, the hyperuniformity concept enables one to identify a static nonequilibrium growing length scale in overcompressed (rapidly compressed) hard-sphere systems as a function of ϕ up to the jammed glassy state.[174,175] This led to the identification of static nonequilibrium growing length scales in supercooled liquids on approaching the glass transition.[177]

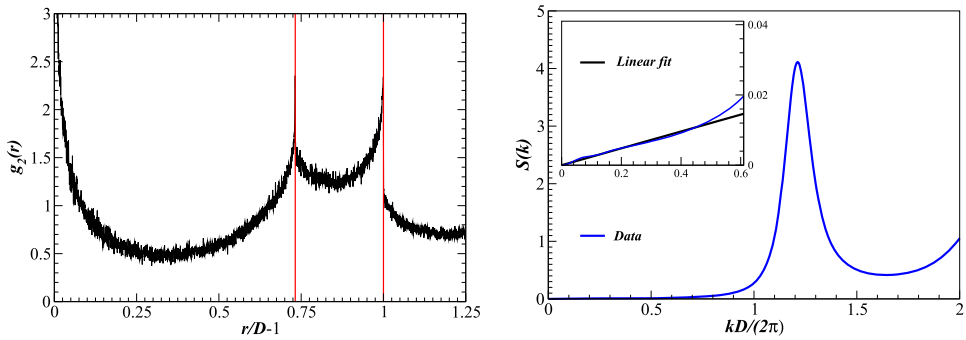

FIG. 8. Pair statistics for packings of spheres of diameter D in the immediate neighborhood of the 3D MRJ state with $\phi \approx 0.64$. Left panel: The pair correlation function $g_2(r)$ versus $r/D - 1$, as taken from Ref. 140. The split second peak, the discontinuity at twice the sphere diameter, and the divergence near contact are clearly visible. Right panel: The corresponding structure factor $S(k)$ as a function of the dimensionless wavenumber $kD/(2\pi)$ for a million-particle packing, as taken from Ref. 70. The inset shows that $S(k)$ tends to zero (within numerical error) linearly in k; hence, an MRJ packing is effectively hyperuniform. Reprinted with permission from A. Donev *et al.*, Phys. Rev. E **71**, 011105 (2005). Copyright 2005 American Physical Society.

The following is a general conjecture from the work of Torquato and Stillinger[71] concerning the conditions under which certain strictly jammed packings are hyperuniform:

Conjecture. Any strictly jammed saturated infinite packing of identical spheres in $\mathbb{R}^d$ *is hyperuniform.*

To date, there is no rigorously known counterexample to this conjecture. Its justification and rigorously known examples are discussed in Refs. 69 and 152.

A recent numerical study of necessarily finite disordered packings calls into question the connection between jamming and perfect hyperuniformity.[178] It is problematic to try to test this conjecture using current packing protocols to construct supposedly disordered jammed states for a variety of reasons. First, we stress that the conjecture eliminates packings that may have a rigid backbone but possess "rattlers"—a subtle point that has not been fully appreciated in numerical investigations.[178–180] Current numerically generated disordered packings that are putatively jammed tend to contain a small concentration of rattlers;[51,70,149,150,181] because of these movable particles, the entire packing cannot be deemed to be "jammed." Moreover, it has recently been shown that various standard packing protocols struggle to reliably create packings that are jammed for even modest system sizes, and yet large system sizes are required in order to access the small-wavenumber regime of the structure factor.[152] Although these packings *appear* to be jammed by conventional tests, rigorous linear-programming jamming tests[121,136] reveal that they are not. Recent evidence has emerged that suggests that deviations from hyperuniformity in putative MRJ packings also can in part be explained by a shortcoming of current numerical protocols that attempt to generate exactly jammed configurations as a result of a type of "critical slowing down:"[152] the packing's collective rearrangements in configuration space become locally confined by high-dimensional "bottlenecks" through which escape is a rare event. Thus, a critical slowing down implies that it becomes increasingly difficult numerically to drive the value of $S(0)$ exactly down to its minimum value of zero if a true jammed critical state could be attained; typically,[70] $S(0) \approx 10^{-4}$. Moreover, the inevitable presence of even a small fraction of rattlers generated by current packing algorithms destroys perfect hyperuniformity. In summary, the difficulty of ensuring jamming in sufficiently large disordered packings as well as the presence of rattlers that degrade hyperuniformity makes it extremely challenging to test the Torquato-Stillinger jamming-hyperuniformity conjecture on disordered jammed packings via current numerical protocols. This raises the possibility that the ideal MRJ packings have no rattlers and provides a challenge to develop packing algorithms that produce large disordered strictly jammed packings that are rattler-free.

A variety of different attributes of MRJ packings generated via the TJ packing algorithm have been investigated in separate studies. In the first paper of a three-part series, Klatt and Torquato[182] ascertained Minkowski correlation functions associated with the Voronoi cells of such MRJ packings and found that they exhibited even stronger anti-correlations than those shown in the standard pair-correlation function.[182] In the second paper of this series,[183] a variety of different correlation functions that arise in rigorous expressions for the effective physical properties of MRJ sphere packings were computed. In the third paper of this series,[184] these structural descriptors were used to estimate effective transport and electromagnetic properties of composites composed of MRJ sphere packings dispersed throughout a matrix phase and showed, among other things, that electromagnetic waves in the long-wavelength limit can propagate without dissipation, as generally predicted in Ref. 185. In a separate study, Ziff and Torquato[186] determined the site and bond percolation thresholds of TJ generated MRJ packings to be $p_c = 0.3116(3)$ and $p_c = 0.2424(3)$, respectively.

Not surprisingly, ensemble methods that produce the "most probable" configurations typically miss interesting extremal points in the order map, such as the locus of points A-A' and the rest of the jamming-region boundary. However, numerical protocols can be devised to yield unusual extremal jammed states. For example, disordered jammed packings can be created in the entire non-trivial range of packing fraction $0.6 < \phi < 0.740\,48\ldots$.[49,131,153] Thus, in Fig. 6, the locus of points along the boundary of the jammed set to the left and right of the MRJ state are achievable. The TJ algorithm[149] was applied to yield disordered strictly jammed packings[153] with ϕ as low as 0.60, which are overconstrained with $Z \approx 6.4$, and hence are more ordered than the MRJ state.

It is well known that lack of "frustration"[20,118] in 2D analogs of 3D computational and experimental protocols that lead to putative RCP states results in packings of identical disks that are highly crystalline, forming rather large triangular coordination domains (grains). Such a 1000-particle packing with $\phi \approx 0.88$ is depicted in the right panel of Fig. 4 and is only collectively jammed at this high density. Because such highly ordered packings are the most probable outcomes for these typical protocols, "entropic measures" of disorder would identify these as the most disordered, a misleading conclusion. Recently, Atkinson *et al.*[151] applied the TJ algorithm to generate relatively large MRJ disk packings with exactly isostatic ($\overline{Z} = 4$) jammed backbones and a packing fraction (including rattlers) of $\phi_{\rm MRJ} \approx 0.827$. Uncovering such disordered jammed packings of identical hard disks challenges the traditional notion that the most probable distribution is necessarily correlated with randomness and hence the RCP state. An analytical formula was derived for MRJ packing fractions of more general 2D packings,[187] yielding the prediction $\phi_{\rm MRJ} = 0.834$ in the monodisperse-disk limit, which is in very good agreement with the aforementioned recent numerical estimate.[151]

F. Packings of spheres with a size distribution

Sphere packings with a size distribution (polydispersity), sometimes called hard-sphere mixtures, exhibit intriguing structural features, some of which are only beginning to be understood. Our knowledge of sphere packings with a size distribution is very limited due in part to the infinite-dimensional parameter space, i.e., all particle size ratios and relative concentrations. It is known, for example, that a relatively small degree of polydispersity can suppress the disorder-order phase transition seen in monodisperse hard-sphere systems (see Fig. 1).[188] Size polydispersity constitutes a fundamental feature of the microstructure of a wide class of dispersions of technological importance, including those involved in composite solid propellant combustion,[63] flow in packed beds,[64] sintering of powders,[65] colloids,[23] and transport and mechanical properties of particulate composite materials.[20] Packings of biological cells in tissues are better modeled by assuming that the spheres have a size distribution.[32,33]

Generally, we allow the spheres to possess a continuous distribution in radius R, which is characterized by a probability density function $f(R)$. The average of any function $w(R)$ is defined by $\langle w(R)\rangle = \int_0^\infty w(R)f(R)dR$. The overall packing fraction ϕ is then defined as

$$\phi = \rho\langle v_1(R)\rangle, \tag{19}$$

where ρ is the total number density and $v_1(R)$ is given by (4). Two continuous probability densities that have been widely used are the Schulz[189] and log-normal[190] distributions. One can obtain the corresponding results for spheres with M discrete different sizes from Eq. (19) by letting

$$f(R) = \sum_{i=1}^{M} \frac{\rho_i}{\rho}\delta(R - R_i), \tag{20}$$

where ρ_i and R_i are the number density and radius of type-i particles, respectively, and ρ is the *total number density*. Therefore, the overall volume fraction using (19) is given by $\phi = \sum_{i=1}^{M} \phi^{(i)}$, where $\phi^{(i)} = \rho_i v_1(R_i)$ is the packing fraction of the ith component.

1. Equilibrium and metastable behavior

The problem of determining the equilibrium phase behavior of hard sphere mixtures is substantially more challenging and richer than that for identical hard spheres, including the possibilities of metastable or stable fluid-fluid and/or solid-solid phase transitions (apart from stable fluid or crystal phases). While much research remains to be done, considerable progress has been made over the years,[61,62,191–212] which we only briefly touch upon here for both additive and nonadditive cases; see Ref. 62 for an overview. In *additive* hard-sphere mixtures, the distance of closest approach between the centers of any two spheres is the arithmetic mean of their diameters. By contrast, in *nonadditive* hard-sphere mixtures, the distance of closest approach between any two spheres is generally no longer the arithmetic mean.

Additive mixtures have been studied both theoretically and computationally. Lebowitz exactly obtained the pair correlation functions of such systems with M components within the Percus-Yevick approximation.[191] Accurate approximate equations of state under liquid conditions have been found for both discrete[194,206] and continuous[195,213] size distributions with additive hard cores. We note that Lado devised an efficient numerical procedure to solve integral equations for the pair correlation function of polydisperse suspensions, yielding the corresponding thermodynamics.[214] Fundamental measure theory can provide useful insights about the phase behavior of hard-sphere mixtures.[197,212] This theory predicts the existence of stable fluid-fluid coexistence for sufficiently large size ratios in additive binary hard-sphere systems, while numerical simulations[61] indicate that such phase separation is metastable with respect to fluid-crystal coexistence and also shows stable solid-solid coexistence. Nonetheless, there is currently no mathematical proof that precludes a fluid-fluid demixing transition in a binary mixture of additive hard spheres for any size ratio and relative composition. In order to quantify fluid-crystal phase coexistence, one must know the densest crystal structure, which is highly nontrivial, especially for large size ratios, although recent progress has been made; see Sec. III F 2.

The Widom-Rowlinson model is an extreme case of nonadditivity in which like species do not interact and unlike species interact via a hard-core repulsion.[192] As the density is increased, this model exhibits a fluid-fluid demixing transition in low dimensions and possesses a critical point that is in the Ising universality class.[202,203] More general nonadditive hard-sphere mixtures in which all spheres interact have been studied. Mixtures of hard spheres with positive nonadditivity (unlike-particle diameters greater than the arithmetic mean of the corresponding like-particle diameters) can exhibit a fluid-fluid demixing transition[61,204,205,207] that belongs to the Ising universality class,[208] while those with negative nonadditivity have tendencies to form alloyed (mixed) fluid phases.[196] For certain binary mixtures of hard sphere fluids with nonadditive diameters, the pair correlation function has been determined in the Percus-Yevick approximation.[193,196]

Fluid phases of hard sphere mixtures, like their monodisperse counterparts, are not hyperuniform. However, multicomponent equilibrium plasmas consisting of nonadditive hard spheres with Coulombic interactions enable one to generate a very wide class of disordered hyperuniform as well as "multihyperuniform"[32] systems at positive temperatures.[215,216]

2. Maximally random jammed states

The study of dense disordered packings of 3D polydisperse additive spheres has received considerable attention.[217–222] However, these investigations did not consider their mechanical stability via our modern understanding of jamming. Not surprisingly, the determination of the MRJ state for an arbitrary polydisperse sphere packing is a challenging open question, but some progress has been made recently, as described below.

Jammed states of polydisperse spheres, whether disordered or ordered, will generally have higher packing fractions when "alloyed" than their monodisperse counterparts. The first investigation that attempted to generate 3D amorphous jammed sphere packings with a polydispersity in size was carried out by Kansal *et al.*[223] using the LS packing algorithm. It was applied to show that disordered binary jammed packings with a small-to-large size ratio α and relative concentration x can be obtained whose packing fractions exceeds 0.64 and indeed can attain $\phi = 0.79$ for $\alpha = 0.1$ (the smallest value considered). Chaudhuri *et al.*[224] numerically generated amorphous 50-50 binary packings with packing fractions in the range $0.648 \le \phi \le 0.662$ for $\alpha = 1.4$. It is notable that Clusel *et al.*[225] carried out a series of experiments to visualize and characterize 3D random packings of frictionless polydisperse emulsion droplets using confocal microscopy.

Until recently, packing protocols that have attempted to produce disordered binary sphere packings have been limited in producing mechanically stable isostatic packings across a broad spectrum of packing fractions. Many previous simulation studies of disordered binary sphere packings have produced packings that are not mechanically stable[218,222,226] and report coordination numbers as opposed to contact numbers. Whereas a coordination number indicates only proximity of two spheres, a contact number reflects mechanical stability and is derived from a jammed network.[44,136]

Using the TJ linear programming packing algorithm,[149] Hopkins *et al.*[227] were recently able to generate high-fidelity strictly jammed, isostatic disordered binary packings with an anomalously large range of packing fractions, $0.634 \le \phi \le 0.829$, with the size ratio restriction $\alpha \ge 0.1$. These packings are MRJ-like due to the nature of the TJ algorithm and the use of RSA initial conditions. Additionally, the packing fractions for certain values of α and x approach those of the corresponding densest known ordered packings.[154,155] These findings suggest that these high-density disordered packings should be good glass formers for entropic reasons and hence may be easy to prepare experimentally. The identification and explicit construction of binary packings with such high packing fractions could have important practical implications for the design of improved solid propellants, concrete, and ceramics. In this connection, a recent study of MRJ binary sphere packings under *confinement* is particularly relevant.[228]

The LS algorithm has been used successfully to generate disordered strictly jammed packings of binary disks[229] with $\phi \approx 0.84$ and $\alpha^{-1} = 1.4$. By explicitly constructing an exponential number of jammed packings of binary disks with densities spanning the spectrum from the accepted amorphous glassy state to the phase-separated crystal, it has been argued[229,230] that there is no "ideal glass transition."[231] The existence of an ideal glass transition remains a hotly debated topic of research.

Simulational[232–234] as well as experimental[235,236] studies of disordered jammed spheres with a size distribution reveal that they are effectively hyperuniform. In such cases, it has been demonstrated that the proper means of investigating hyperuniformity is through the spectral density $\tilde{\chi}_V(\mathbf{k})$,[232,233] which is defined by condition (14).

3. Densest packings

The densest packings of spheres with a size distribution are of great interest in crystallography, chemistry, and materials science. It is notable that the densest packings of hard-sphere mixtures are intimately related to high-pressure phases of molecular systems, including intermetallic compounds[66] and solid rare-gas compounds[67] for a range of temperatures.

Except for trivial space-filling structures, there are no provably densest packings when the spheres possess a size distribution, which is a testament to the mathematical challenges that they present. We begin by noting some rigorous bounds on the maximal packing fraction of packings of spheres with M different radii $R_1, R_2, \ldots, R_M$ in $\mathbb{R}^d$. Specifically, the overall maximal packing fraction $\phi_{\max}^{(M)}$ of such a general mixture in $\mathbb{R}^d$ [where ϕ is defined by (19) with (20)] is bounded from the above and below in terms of the maximal packing fraction $\phi_{\max}^{(1)}$ for a monodisperse packing in the infinite-volume limit,[20]

$$\phi_{\max}^{(1)} \le \phi_{\max}^{(M)} \le 1 - (1 - \phi_{\max}^{(1)})^M. \tag{21}$$

The lower bound corresponds to the case when the M components completely demix, each at the density $\phi_{\max}^{(1)}$. The upper bound corresponds to an ideal sequential packing process for arbitrary M in which one takes the limits $R_1/R_2 \to 0$, $R_2/R_3 \to 0, \ldots, R_{M-1}/R_M \to 0$.[20] Specific *nonsequential* protocols (algorithmic or otherwise) that can generate structures that approach the upper bound (21) for arbitrary values of M are currently unknown, and thus, the development of such protocols is an open area of research. We see that in the limit $M \to \infty$, the upper bound approaches unity, corresponding to space-filling polydisperse spheres with an infinitely wide separation in sizes[237] or a continuous size distribution with sizes ranging to infinitesimally small.[20]

Even the characterization of the densest jammed *binary* sphere packings offers great challenges and is very far from completion. Here we briefly review some work concerning such packings in two and three dimensions. Ideally, it is desired to obtain $\phi_{\max}$ as a function of α and x. In practice, we have a sketchy understanding of the surface defined by $\phi_{\max}(\alpha, x)$.

Among the 2D and 3D cases, we know most about the determination of the maximally dense binary packings in $\mathbb{R}^2$. Fejes Tóth[167] reported a number of candidate maximally dense packings for certain values of the radii ratio in the range $\alpha \geq 0.154\,701\ldots$. Maximally dense binary disk packings have been also studied to determine the stable crystal phase diagram of such alloys.[238] The determination of $\phi_{\max}$ for sufficiently small α amounts to finding the optimal arrangement of the small disks within a *tricusp*: the nonconvex cavity between three close-packed large disks. A particle-growth Monte Carlo algorithm was used to generate the densest arrangements of a fixed number of small identical disks within such a tricusp.[239] All of these results can be compared to a relatively tight upper bound on $\phi_{\max}$ given by[240]

$$\phi_{\max} \leq \phi_U = \frac{\pi\alpha^2 + 2(1-\alpha^2)\sin^{-1}\left(\frac{\alpha}{1+\alpha}\right)}{2\alpha(1+2\alpha)^{1/2}}. \tag{22}$$

Inequality (22) also applies to general multicomponent packings, where α is taken to be the ratio of the smallest disk radius to the largest one.

There is great interest in finding the densest binary sphere packings in $\mathbb{R}^3$ in physical sciences because of their relationship to binary crystal alloys found in molecular systems; see Refs. 155 and 241 as well as the references therein for details and some history. Past efforts to identify such optimal packings have employed simple crystallographic techniques (filling the interstices in uniform 3D tilings of space with spheres of different sizes) and algorithmic methods, e.g., Monte Carlo calculations and a genetic algorithm.[242,243] However, these methods have achieved only limited success, in part due to the infinite parameter space that is involved. When using traditional algorithms, difficulties result from the enormous number of steps required to escape from local minima in the "energy" (negative of the packing fraction). Hopkins *et al.*[154,155] have presented the most comprehensive determination to date of the "phase diagram" for the densest binary sphere packings via the TJ linear-programming algorithm.[149] In Ref. 155, 19 distinct crystal alloys (compositions of large and small spheres spatially mixed within a fundamental cell) were identified, including 8 that were unknown at the time. Using the TJ algorithm, they were always able to obtain either the densest previously known alloy or the denser ones. These structures may correspond to currently unidentified stable phases of certain binary atomic and molecular systems, particularly at high temperatures and pressures.[66,67] Reference 155 provides details about the structural characteristics of these densest-known binary sphere packings.

IV. PACKING SPHERES IN HIGH DIMENSIONS

Sphere packings in four- and higher-dimensional Euclidean spaces are of great interest in the physical and mathematical sciences; see Refs. 38, 44, 52, 68, 111, 156, 157, 173, and 244–259. Physicists have studied high-dimensional packings to gain insight into liquid, crystal, and glassy states of matter in lower dimensions.[52,173,245,246,248,251,252,255,256,260] Finding the densest packings in arbitrary dimension in Euclidean and compact spaces is a problem of long-standing interest in discrete geometry.[37,38,261,262] Remarkably, the optimal way of sending digital signals over noisy channels corresponds to the densest sphere packing in a high-dimensional space.[37,40] These "error-correcting" codes underlie a variety of systems in digital communications and storage, including compact disks, cell phones, and the Internet.

A. Equilibrium and metastable phase behavior

The properties of equilibrium and metastable states of hard spheres have been studied both theoretically and computationally in spatial dimensions greater than three.[173,245,255–257,263,264] This includes the evaluation of various virial coefficients across dimensions,[263,264] as well as the pressure along the liquid, metastable, and crystal branches,[173,251,255–257] especially for $d = 4$, 5, 6, and 7. Using the LS packing algorithm, Skoge *et al.*[173] numerically estimated the freezing and melting packing fractions for the equilibrium hard-sphere fluid-solid transition, $\phi_F \simeq 0.32$ and $\phi_M \simeq 0.39$, respectively, for $d = 4$, and $\phi_F \simeq 0.19$ and $\phi_M \simeq 0.24$, respectively, for $d = 5$. These authors showed that nucleation appears to be strongly suppressed with increasing dimension. The same conclusion was subsequently reached in a study by van Meel *et al.*[256] Finken, Schmidt, and Löwen[265] used a variety of approximate theoretical methods to show that equilibrium hard spheres have a first-order freezing transition for dimensions as high as $d = 50$.

Any disordered packing in which the pair correlation function at contact, $g_2(D^+)$, is bounded (such as equilibrium hard spheres) induces a power-law decay in the structure factor $S(k)$ in the limit $k \to \infty$ for any dimension d given by

$$S(k) \sim 1 - \frac{2^{\frac{3d+1}{2}}\Gamma(1+d/2)\phi g_2(D^+)}{\sqrt{\pi}(kD)^{\frac{d+1}{2}}}\cos[kD - (d+1)\pi/4]\,. \tag{23}$$

There is a remarkable duality between the equilibrium hard-hypersphere (hypercube) fluid system in $\mathbb{R}^d$ and the continuum percolation model of overlapping hyperspheres (hypercubes) in $\mathbb{R}^d$. In particular, the pair connectedness function of the latter is to a good approximation equal to the negative of the total correlation function of the former evaluated at *negative* density.[266] This mapping becomes exact for $d = 1$ and in the large-d limit.

B. Nonequilibrium disordered packings via sequential addition

In Sec. III B 2, we noted that the "ghost" RSA packing[111] is a disordered but *unsaturated* packing construction whose n-particle correlation functions are known exactly and rigorously achieves the infinite-time packing fraction $\phi = 2^{-d}$ for any d; see Fig. 3 for a 2D realization of such a packing.

Saturated RSA sphere packings have been numerically generated and structurally characterized for dimensions up through $d = 6$ (Ref. 96). A more efficient numerical procedure was devised to produce such packings for dimensions up through $d = 8$ (Ref. 97). The current best estimates of the

maximal saturation packing fraction ϕ_s for $d = 4, 5, 6, 7$, and 8 are $0.260\,078\,1 \pm 0.000\,003\,7$, $0.170\,776\,1 \pm 0.000\,004\,6$, $0.109\,302 \pm 0.000\,019$, $0.068\,404 \pm 0.000\,016$, and $0.042\,30 \pm 0.000\,21$, respectively.[97] These are lower than the corresponding MRJ packing fractions in those dimensions (see Sec. IV C). The quantity ϕ_s apparently scales as $d \cdot 2^{-d}$ or possibly $d \cdot \ln(d) \cdot 2^{-d}$ for large d; see Refs. 96 and 97. While saturated RSA packings are nearly but not exactly hyperuniform,[96] as d increases, the degree of hyperuniformity increases and pair correlations markedly diminish,[97] consistent with the decorrelation principle,[68] which is described in Sec. IV E.

C. Maximally random jammed states

Using the LS algorithm, Skoge *et al.*[173] generated and characterized MRJ packings in four, five, and six dimensions. In particular, they estimated the MRJ packing fractions, finding $\phi_{\rm MRJ} \simeq 0.46, 0.31$, and 0.20 for $d = 4, 5$, and 6, respectively. To a good approximation, the MRJ packing fraction obeys the scaling form $\phi_{\rm MRJ} = c_1 2^{-d} + c_2 d \cdot 2^{-d}$, where $c_1 = -2.72$ and $c_2 = 2.56$, which appears to be consistent with a high-dimensional asymptotic limit, albeit with different coefficients. The dominant large-d density scaling $d \cdot 2^{-d}$ is supported by theoretical studies.[68,258,267,268] Skoge *et al.*[173] also determined the MRJ pair correlation function $g_2(r)$ and structure factor $S(k)$ for these states and found that short-range ordering appreciably decreases with increasing dimension, consistent with the *decorrelation principle*.[68] This implies that, in the limit $d \to \infty$, $g_2(r)$ tends to unity for all r outside the hard-core, except for a Dirac delta function at contact due to the jamming constraint.[68] As for $d = 3$ (where $\phi_{\rm MRJ} \simeq 0.64$), the MRJ packings were found to be isostatic and hyperuniform and have a power-law divergence in $g_2(r)$ at contact, $g_2(r) \sim 1/(r - D)^{\alpha}$ with $\alpha \approx 0.4$ as r tends to D^+. Across dimensions, the cumulative number of neighbors was shown to equal the *kissing* (contact) number of the conjectured densest packing close to where $g_2(r)$ has its first minimum. Disordered jammed packings were also simulated and studied in dimensions 7-10; see Ref. 269.

D. Maximally dense sphere packings

The sphere packing problem seeks to answer the following question:[37] Among all packings of congruent spheres in $\mathbb{R}^d$, what is the maximal packing fraction $\phi_{\rm max}$ and the corresponding arrangements of the spheres? Until 2017, the optimal solutions were known only for the first three space dimensions.[43] For $d = 2$ and $d = 3$, these are the triangular lattice (A_2) with $\phi_{\rm max} = \pi/\sqrt{12} = 0.906\,899\ldots$ and checkerboard (fcc) lattice (D_3) and its stacking variants with $\phi_{\rm max} = \pi/\sqrt{18} = 0.740\,48\ldots$, respectively. We now know the optimal solutions in two other space dimensions; namely, the E_8 and Λ_{24} lattices are the densest packings among all possible packings in $\mathbb{R}^8$ and $\mathbb{R}^{24}$, respectively; see Refs. 261 and 262. For $4 \le d \le 9$, the densest known packings are (Bravais) lattice packings.[37] The "checkerboard" lattice D_d is believed to be optimal in $\mathbb{R}^4$ and $\mathbb{R}^5$. Interestingly, the non-lattice (periodic) packing P_{10c} (with 40 spheres per fundamental cell) is the densest known packing in $\mathbb{R}^{10}$, which is the lowest dimension in which the best known packing is not a (Bravais) lattice.

Table I lists the densest known or optimal sphere packings in $\mathbb{R}^d$ for selected d. For the first three space dimensions, the optimal sphere-packing solutions (or their "dual" solutions) are directly related to the best known solutions of the *number-variance* problem[71,72] as well as of two other well-known problems in discrete geometry: the *covering* and *quantizer* problems,[37,270] but such relationships may or may not exist for $d \ge 4$, depending on the peculiarities of the dimensions involved.[271]

The TJ linear-programming packing algorithm was adapted by Marcotte and Torquato[156] to determine the densest lattice packing (one particle per fundamental cell) in some high dimension. These authors applied it for $2 \le d \le 19$ and showed that it was able to rapidly and reliably discover the densest known lattice packings without *a priori* knowledge of their existence. It was found to be appreciably faster than the previously known algorithms at that time.[272,273] The TJ algorithm was used to generate an ensemble of isostatic jammed hard-sphere lattices and study the associated pair statistic and force distributions.[157] It was shown that this special ensemble of lattice-sphere packings retains many of the crucial structural features of the classical hard-sphere model.

It is noteworthy that for sufficiently large d, lattice packings are most likely not the densest (see Fig. 9), but it becomes increasingly difficult to find explicit dense packing constructions as d increases. Indeed, the problem of finding the shortest lattice vector in a particular lattice packing grows super-exponentially with d and is in the class of NP-hard (nondeterministic polynomial-time hard) problems.[274]

For large d, the best that one can do theoretically is to devise upper and lower bounds on $\phi_{\rm max}$.[37] The *nonconstructive* lower bound of Minkowski[275] established the existence of

TABLE I. The densest known or optimal sphere packings in $\mathbb{R}^d$ for selected d. For each packing, we provide the packing fraction ϕ and kissing number Z. Except for the non-lattice packing P_{10c} in $\mathbb{R}^{10}$, all of the other densest known packings listed in this table are lattice packings: $\mathbb{Z}$ is the integer lattice, A_2 is the triangular lattice, D_d is the checkerboard lattice (a generalization of the fcc lattice), E_d is one of the root lattices, and Λ_d is the laminated lattice. For $d = 8$ and $d = 24$, it has recently been proved that E_8 and Λ_{24} are optimal among all packings, respectively; see Refs. 261 and 262. The reader is referred to Ref. 37 for additional details.

d	Packing	Packing fraction, ϕ	Kissing number, Z
1	$\mathbb{Z}$	1	2
2	A_2	$\pi/\sqrt{12} = 0.906\,8\ldots$	6
3	D_3	$\pi/\sqrt{18} = 0.740\,4\ldots$	12
4	D_4	$\pi^2/16 = 0.616\,8\ldots$	24
5	D_5	$2\pi^2/(30\sqrt{2}) = 0.465\,2\ldots$	40
6	E_6	$3\pi^2/(144\sqrt{3}) = 0.372\,9\ldots$	72
7	E_7	$\pi^3/105 = 0.295\,2\ldots$	126
8	E_8	$\pi^4/384 = 0.253\,6\ldots$	240
9	Λ_9	$2\pi^4/(945\sqrt{2}) = 0.145\,7\ldots$	272
10	P_{10c}	$\pi^5/3\,072 = 0.099\,61\ldots$	372
16	Λ_{16}	$\pi^8/645\,120 = 0.014\,70\ldots$	4 320
24	Λ_{24}	$\pi^{12}/479\,001\,600 = 0.001\,929\ldots$	196 360

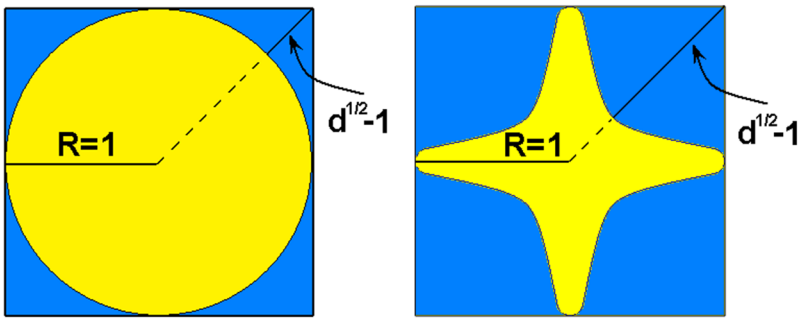

FIG. 9. Lattice packings in sufficiently high dimensions are not dense because the "holes" (space exterior to the spheres) eventually dominates the space $\mathbb{R}^d$ and hence become *unsaturated*.[37] For illustration purposes, we consider the hypercubic lattice $\mathbb{Z}^d$. Left panel: A fundamental cell of $\mathbb{Z}^d$ represented in two dimensions. The distance between the point of intersection of the longest diagonal in the hypercube with the hypersphere boundary and the vertex of the cube along this diagonal is given by $\sqrt{d} - 1$ for a sphere of unit radius. This means that $\mathbb{Z}^d$ already becomes unsaturated at $d = 4$. Placing an additional sphere in $\mathbb{Z}^4$ doubles the density of $\mathbb{Z}^4$ and yields the four-dimensional checkerboard lattice packing D_4, which is believed to be the optimal packing in $\mathbb{R}^4$. Right panel: A schematic "effective" distorted representation of the hypersphere within the hypercubic fundamental cell for large d, illustrating that the volume content of the hypersphere relative to the hypercube rapidly diminishes asymptotically. Indeed, the packing fraction of $\mathbb{Z}^d$ is given by $\phi = \pi^{d/2}/(\Gamma(1 + d/2)2^d)$. Indeed, the checkerboard lattice D_d with packing fraction $\phi = \pi^{d/2}/(\Gamma(1 + d/2)2^{(d+2)/2})$ becomes suboptimal in relatively low dimensions because it also becomes dominated by larger and larger holes as d increases. Reprinted with permission from S. Torquato and F. H. Stillinger, Rev. Mod. Phys. **82**, 2633 (2010). Copyright 2010 American Physical Society.

reasonably dense lattice packings. He found that the maximal packing fraction $\phi^L_{\max}$ among all lattice packings for $d \geq 2$ satisfies

$$\phi^L_{\max} \geq \frac{\zeta(d)}{2^{d-1}}, \tag{24}$$

where $\zeta(d) = \sum_{k=1}^{\infty} k^{-d}$ is the Riemann zeta function. Note that for large values of d, the asymptotic behavior of the Minkowski lower bound is controlled by 2^{-d}. Since 1905, many extensions and generalizations of the lower bound (24) have been derived,[37,276–278] but none of these investigations have been able to improve upon the dominant exponential term 2^{-d}; they instead only improve on the latter by a factor linear in d.

It is trivial to prove that the packing fraction of a *saturated* packing of congruent spheres in $\mathbb{R}^d$ satisfies[111]

$$\phi \geq \frac{1}{2^d} \tag{25}$$

for all d. This "greedy" bound (25) has the same dominant exponential term as Minkowski's bound (24).

Nontrivial upper bounds on $\phi_{\max}$ in $\mathbb{R}^d$ for any d have been derived.[38,39,279–281] The linear-programming (LP) upper bounds from the work of Cohn and Elkies[38] provides the basic framework for proving the best known upper bounds on $\phi_{\max}$ for dimensions in the range $4 \leq d \leq 36$. Recently, these LP bounds have been used to prove that no packings in $\mathbb{R}^8$ and $\mathbb{R}^{24}$ have densities that can exceed those of the E_8 (Ref. 261) and L_{24} (Ref. 262) lattices, respectively. Kabatiansky and Levenshtein[281] found the best asymptotic upper bound, which in the limit $d \to \infty$ yields $\phi_{\max} \leq 2^{-0.5990d}$, proving that the maximal packing fraction tends to zero in the limit $d \to \infty$. This rather counterintuitive high-dimensional property of sphere packings can be understood by recognizing that almost all of the volume of a d-dimensional sphere for large d is concentrated near the sphere surface.

E. Are disordered packings the densest in high dimensions?

Since 1905, many extensions and generalizations of Minkowski's bound have been derived,[37] but none of them have improved upon the dominant exponential term 2^{-d}. The existence of the *unjammed* disordered ghost RSA packing[111] (Sec. III B 2) that rigorously achieves a packing fraction of 2^{-d} strongly suggests that Bravais-lattice packings (which are almost surely unsaturated in sufficiently high d) are far from optimal for large d.

Torquato and Stillinger[68] employed a plausible conjecture that strongly supports the counterintuitive possibility that the densest sphere packings for sufficiently large d may be disordered or at least possess fundamental cells whose size and structural complexity increase with d. They did so using the so-called g_2-invariant optimization procedure that maximizes ϕ associated with a radial "test" pair correlation function $g_2(r)$ to provide the putative exponential improvement on Minkowski's 100-year-old bound on $\phi_{\max}$. Specifically, a *g_2-invariant process*[267] is the one in which the functional form of a "test" pair correlation $g_2(\mathbf{r})$ function remains invariant as density varies, for all $\mathbf{r}$, over the range of packing fractions $0 \leq \phi \leq \phi_*$ subject to the satisfaction of the non-negativity of the structure factor $S(\mathbf{k})$ and $g_2(\mathbf{r})$. When there exist sphere packings with a g_2 satisfying these conditions in the interval $[0, \phi_*]$, then one has the lower bound on the maximal packing fraction given by

$$\phi_{\max} \geq \phi_*. \tag{26}$$

Torquato and Stillinger[68] conjectured that a test function $g_2(\mathbf{r})$ is a pair-correlation function of a translationally invariant disordered sphere packing in $\mathbb{R}^d$ for $0 \leq \phi \leq \phi_*$ for sufficiently large d if and only if the non-negativity conditions on $S(\mathbf{k})$ and $g_2(\mathbf{r})$ are satisfied. The *decorrelation principle*,[68] among other results,[44,253,259] provides justification for the conjecture. This principle states that unconstrained correlations in disordered sphere packings vanish asymptotically in high dimensions and that the g_n for any $n \geq 3$ can be inferred entirely (up to small errors) from the knowledge of ρ and g_2.[68] This is vividly exhibited by the exactly solvable ghost RSA packing process[111] as well as by computer simulations of high-dimensional MRJ[173] and RSA[250] packings. Interestingly, this optimization problem is the *dual* of the infinite-dimensional linear program

(LP) devised by Cohn and Elkies[249] to obtain upper bounds on $\phi_{\max}$.

Using a particular test pair correlation corresponding to a disordered sphere packing, Torquato and Stillinger[68] found a conjectural lower bound on $\phi_{\max}$ that is controlled by $2^{-(0.77865\ldots)d}$, thus providing the first putative exponential improvement on Minkowski's lower bound (24). Scardicchio, Stillinger, and Torquato[253] studied a wider class of test functions (corresponding to disordered packings) that lead to precisely the same putative exponential improvement on Minkowski's lower bound, and therefore, the asymptotic form $2^{-(0.77865\ldots)d}$ is much more general and robust than previously surmised.

Zachary and Torquato[282] studied, among other quantities, pair statistics of high-dimensional generalizations of the periodic 2D kagomé and 3D diamond crystal structures. They showed that the decorrelation principle is remarkably already exhibited in these periodic crystals in low dimensions, suggesting that it applies for any sphere packing in high dimensions, whether disordered or not. This conclusion was bolstered in a subsequent study by Andreanov, Scardicchio, and Torquato[259] who showed that strictly jammed lattice sphere packings visibly decorrelate as d increases in relatively low dimensions.

F. Remarks on packing problems in non-Euclidean spaces

Particle packing problems in non-Euclidean (curved) spaces arise in a variety of fields, including physics,[283–285] biology,[34,286–289] communication theory,[37] and geometry.[37,41,55,290,291] While a comprehensive overview of this topic is beyond the scope of this review, it is useful to highlight here some of the developments for the interested reader. We will limit the discussion to sphere packings on the positively curved unit sphere $S^{d-1} \subset \mathbb{R}^d$. The reader is referred to the review by Torquato and Stillinger[44] for some discussion of negatively curved hyperbolic space $\mathbb{H}^d$.

Recall that the *kissing* number Z is the number of spheres of unit radius that simultaneously touch a unit sphere S^{d-1}.[37] The kissing number problem asks for the maximal kissing number Z_{max} in $\mathbb{R}^d$. The determination of the maximal kissing number in $\mathbb{R}^3$ spurred a famous debate between Issac Newton and David Gregory in 1694. The former correctly thought the answer was 12, but the latter wrongly believed that it was 13. The maximal kissing number Z_{max} for $d > 3$ is only known in dimensions four,[292] eight,[293,294] and twenty four.[293,294]

A packing of congruent spherical caps on the unit sphere S^{d-1} in $\mathbb{R}^d$ yields a *spherical code* consisting of the centers of the caps.[37] A spherical code is optimal if the minimal distance (smallest angular separation between distinct points in the code) is as large as possible. The reader is referred to the paper by Cohn and Kumar[41] and the references therein for some developments in the mathematics literature. Interestingly, the jamming of spherical codes in a variety of dimensions has been investigated.[55] It is noteworthy that some optimal spherical codes[295] are related to the densest local packing of spheres around a central sphere.[296,297]

V. PACKINGS OF NONSPHERICAL PARTICLES

The packing characteristics of equilibrium phases and jammed states of packings of nonspherical particles are considerably richer than their spherical counterparts.[80,133,134,139,143,144,147,148,272,298–336] This is due to the fact that nonsphericity of the particle shape introduces rotational degrees of freedom not present in sphere packings. Our primary interest is in simple 3D convex shapes, such as ellipsoids, superballs, spherocylinders, and polyhedra, although we remark on more complex shapes, such as concave particles as well as congruent ring tori, which are multiply connected nonconvex bodies of genus 1. Organizing principles to characterize and classify very dense possibly jammed packings of nonspherical particles in terms of shape symmetry of the particles[24,147,321] are discussed in Sec. V D 5.

A. Simple nonspherical convex shapes

1. Ellipsoids

One simple generalization of the sphere is an ellipsoid, the family of which is a continuous deformation of a sphere. A d-dimensional ellipsoid in $\mathbb{R}^d$ is a centrally symmetric body occupying the region

$$\left(\frac{x_1}{a_1}\right)^2 + \left(\frac{x_2}{a_2}\right)^2 + \cdots + \left(\frac{x_d}{a_d}\right)^2 \le 1, \tag{27}$$

where x_i ($i = 1, 2, \ldots, d$) are the Cartesian coordinates and a_i are the semi-axes of the ellipsoid. Thus, we see that an ellipsoid is an *affine* (linear) transformation of the sphere.

2. Superballs

A d-dimensional *superball* in $\mathbb{R}^d$ is a centrally symmetric body occupying the region

$$|x_1|^{2p} + |x_2|^{2p} + \cdots + |x_d|^{2p} \le 1, \tag{28}$$

where x_i ($i = 1, \ldots, d$) are the Cartesian coordinates and $p \ge 0$ is the *deformation parameter* (not pressure, as denoted in Sec. III A), which controls the extent to which the particle shape has deformed from that of a d-dimensional sphere ($p = 1$). Thus, superballs constitute a large family of both convex ($p \ge 1/2$) and concave ($0 < p < 1/2$) particles (see Fig. 10). A "superdisk," which is the designation in the 2D case, possesses square symmetry. As p moves away from unity, two families of superdisks with square symmetry can be obtained depending on whether $p < 1$ or $p > 1$. When $p < 1/2$, the superdisk is concave; see Ref. 145.

3. Spherocylinder

A d-dimensional spherocylinder in $\mathbb{R}^d$ consists of a cylinder of length L and radius R capped at both ends by hemispheres of radius R and therefore is a centrally symmetric convex particle. Its volume V_{SC} for $d \ge 2$ is given by

$$V_{SC} = \frac{\pi^{(d-1)/2} R^{d-1}}{\Gamma(1 + (d-1)/2)} L + \frac{\pi^{d/2} R^d}{\Gamma(1 + d/2)}. \tag{29}$$

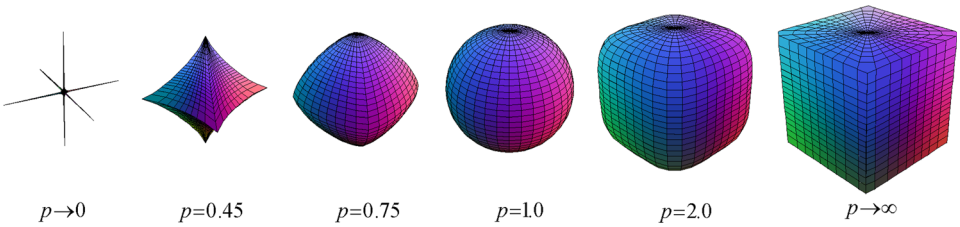

FIG. 10. Superballs with different values of the deformation parameter p. We note that p = 0, 1/2, 1, and ∞ correspond to a 3D cross, regular octahedron, sphere, and cube, respectively.

When L = 0, a d-dimensional spherocylinder reduces to a d-dimensional sphere of radius R. Figure 11 shows 3D examples.

4. Polyhedra

The Platonic solids (mentioned in Plato's Timaeus) are convex polyhedra with faces composed of congruent convex regular polygons. There are exactly five such solids: the tetrahedron (P1), icosahedron (P2), dodecahedron (P3), octahedron (P4), and cube (P5) (see Fig. 12). Note that viral capsids often have icosahedral symmetry; see, for example, Ref. 289.

An Archimedean solid is a highly symmetric semi-regular convex polyhedron composed of two or more types of regular polygons meeting in identical vertices. The thirteen Archimedean solids are depicted in Fig. 13. This typical enumeration does not count the chiral forms (not shown) of the snub cube (A3) and snub dodecahedron (A4). The remaining 11 Archimedean solids are non-chiral (i.e., each solid is superposable on its mirror image), and the only non-centrally symmetric one among these is the truncated tetrahedron.

It is noteworthy that the tetrahedron (P1) and the truncated tetrahedron (A1) are the only Platonic and non-chiral Archimedean solids, respectively, which are not *centrally symmetric*. We will see that the central symmetry of the majority of the Platonic and Archimedean solids (P2–P5, A2–A13) distinguish their dense packing arrangements from those of the non-centrally symmetric ones (P1 and A1) in a fundamental way.

B. Equilibrium and metastable phase behavior

Hard nonspherical particles exhibit a richer phase diagram than that of hard spheres because the former can possess different degrees of translational and orientational order; see Refs. 62, 80, 298, 300, 302, 306, 308, 310, 316, 317, 319, 323, 324, 327–329, 331, 334, and 337–343. Nonspherical particle systems can form isotropic liquids, a variety of liquid crystal phases, rotator crystals, and solid crystals. Particles in liquid phases have neither translational nor orientational order. Examples of liquid crystal states include a nematic phase in which the particles are aligned (i.e., with orientational order), while the system lacks any long-range translational order and a smectic phase in which the particles have ordered orientations and possess translational order in one direction. A rotator (or plastic) phase is the one in which particles possess translational order but can rotate freely. Solid crystals are characterized by both the translational and orientational order.

FIG. 11. Three-dimensional spherocylinders composed of a cylinder with length L, caped at both ends with hemispheres with radius R. Left panel: A spherocylinder with aspect ratio L/R = 1. Right panel: A spherocylinder with aspect ratio L/R = 5.

Ordering transitions in systems of hard nonspherical particles are entropically driven; i.e., the stable phase is determined by a competition between translational and orientational entropies. This principle was first established in the pioneering work of Onsager,[298] where it was shown that needle-like shapes exhibit a liquid-nematic phase transition at low densities because in the nematic phase the drop in orientational entropy is offset by the increase in translational entropy, i.e., the available space for any needle increases as the needle tends to align.

The stable phase formed by systems of hard-nonspherical particles is influenced by its symmetry and surface smoothness, which in turn determines the overall system entropy. Here we briefly highlight 3D numerical studies that use Monte Carlo methods and/or free-energy calculations to determine the phase diagrams. Spheroids exhibit not only fluid, solid crystal, and nematic phases for some aspect ratios but also rotator phases for nearly spherical particle shapes at intermediate densities.[328,337] Hard "lenses" (common volume to two overlapping identical spheres) have a qualitatively similar phase diagram to hard oblate spheroids, but differences between them are more pronounced in the high-density crystal phase up to the densest-known packings.[334] Spherocylinders exhibit five different possible phases, depending on the packing fraction and aspect ratio: isotropic fluid, smectic, nematic, rotator, and solid crystal phases.[308] Apart from fluid and crystal phases, superballs can form rotator phases at intermediate densities.[316,327] Systems of tetragonal parallelepipeds can exhibit liquid-crystalline and cubatic phases, depending on the aspect ratio and packing fraction.[306] Various convex space-filling polyhedra (including truncated octahedron, rhombic dodecahedron, and two types of prisms and cube) possess unusual liquid-crystalline and rotator-crystalline phases at intermediate packing fractions.[319] Interestingly, vacancies in hard cube systems can stabilize the crystal phase.[342] Truncated cubes exhibit a rich diversity in crystal structures that depend sensitively on the amount of truncation.[329] A study of a wide class of polyhedra revealed

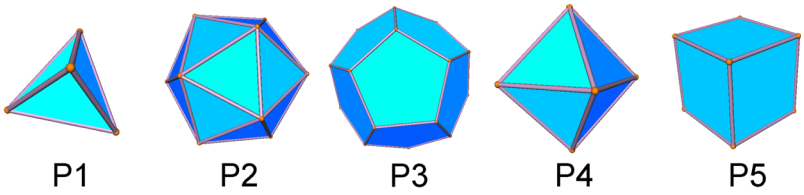

FIG. 12. The five Platonic solids: tetrahedron (P1), icosahedron (P2), dodecahedron (P3), octahedron (P4), and cube (P5).

that entropy maximization favors mutual alignment of particles along their facets.[324] By analytically constructing the densest known packings of congruent Archimedean truncated tetrahedra (which nearly fill all of space), the melting properties of such systems were examined by decompressing this densest packing and equilibrating them.[317] A study of the entire phase diagram of truncated tetrahedra showed that the system undergoes two first-order phase transitions as the density increases: first a liquid-solid transition and then a solid-solid transition.[331]

C. Maximally random jammed states

The fact that M&M candies (spheroidal particles with aspect ratio $\alpha \approx 1.9$) were shown experimentally to randomly pack more densely than spheres ($\phi \approx 0.66$) motivated the development of a modified LS algorithm[143,144] to obtain frictionless MRJ-like packings with even higher densities for other aspect ratios. This included nearly spherical ellipsoids with $\phi \approx 0.74$,[133,134] i.e., packing fractions approaching those of the densest 3D sphere packings. Note that these other densest MRJ packings are realizable experimentally.[139]

Figure 14 shows separate plots of ϕ and mean contact number $\overline{Z}$ as a function of α as predicted by the more refined simulations of Donev *et al.*[134] Each plot shows a cusp (i.e., non-differentiable) minimum at the sphere point, and ϕ versus aspect ratio α possesses a density maximum. The existence of a cusp at the sphere point runs counter to the conventional expectation that for "generic" (disordered) jammed frictionless particles, the total number of (independent) constraints equals the total number of degrees of freedom d_f, which has been referred to as the *isostatic* conjecture.[344] This conjecture implies a mean contact number $\overline{Z} = 2d_f$, where $d_f = 2$ for disks, $d_f = 3$ for ellipses, $d_f = 3$ for spheres, $d_f = 5$ for spheroids, and $d_f = 6$ for general ellipsoids. Since d_f increases discontinuously with the introduction of rotational degrees of freedom as one makes the particles nonspherical, the isostatic conjecture predicts that $\overline{Z}$ should have a jump increase at aspect ratio $\alpha = 1$ to a value of $\overline{Z} = 12$ for a general ellipsoid. Such a discontinuity was not originally observed by Donev *et al.*,[133] rather, they found that jammed ellipsoid packings are *hypostatic* (or sub-isostatic), $\overline{Z} < 2d_f$, near the sphere point, and only become nearly isostatic for large aspect ratios. In fact, the isostatic conjecture is only rigorously true for amorphous sphere packings after removal of rattlers; generic nonspherical-particle packings should generally be hypostatic.[134,345] It has been rigorously shown that packings of nonspherical particles are generally not jammed to first order in the "jamming gap" δ [see Sec. III C 2] but are jammed to second order in δ due to curvature deviations from the sphere.[134] In striking contrast with MRJ sphere packings, the rattler concentrations of the MRJ ellipsoid packings appear practically to vanish outside of some small neighborhood of the sphere point.[134] The reader is referred to recent work on hypostatic jammed 2D packings of noncircular particles.[336]

Jiao, Stillinger, and Torquato[311] have computed the packing fraction ϕ_{MRJ} of MRJ packings of binary superdisks in $\mathbb{R}^2$ and identical superballs in $\mathbb{R}^3$. They found that ϕ_{MRJ} increases dramatically and nonanalytically as one moves away from the circular-disk or sphere point ($p = 1$). Moreover, these disordered packings were shown to be *hypostatic*. Hence,

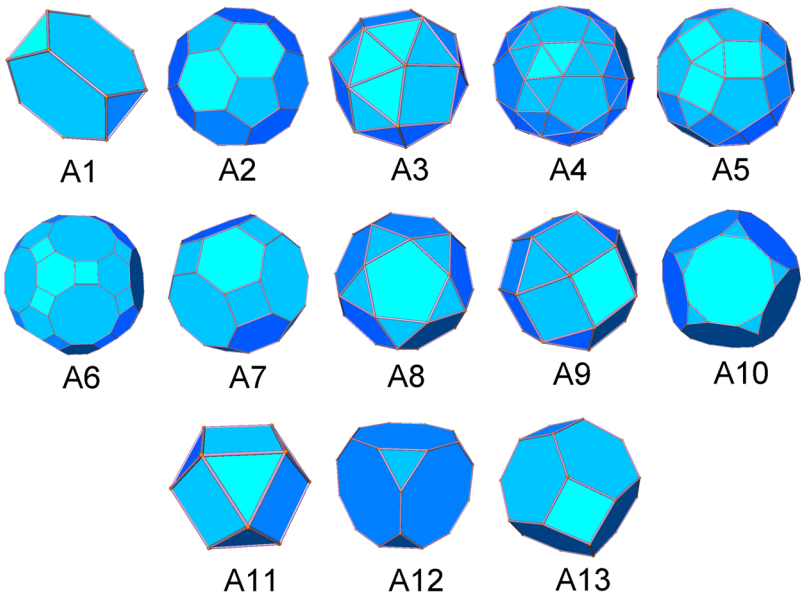

FIG. 13. The thirteen Archimedean solids: truncated tetrahedron (A1), truncated icosahedron (A2), snub cube (A3), snub dodecahedron (A4), rhombicosidodecahedron (A5), truncated icosidodecahedron (A6), truncated cuboctahedron (A7), icosidodecahedron (A8), rhombicuboctahedron (A9), truncated dodecahedron (A10), cuboctahedron (A11), truncated cube (A12), and truncated octahedron (A13).

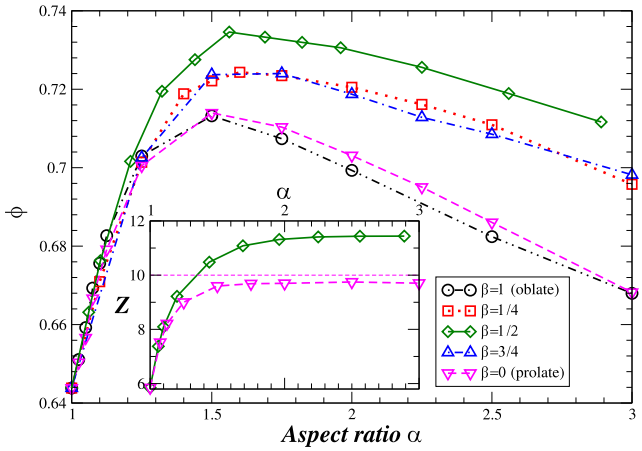

FIG. 14. Packing fraction ϕ versus aspect ratio α for MRJ packings of 10 000 ellipsoids, as obtained in Ref. 134. The semi-axes here are 1, α^β, and α. The inset shows the mean contact number $\overline{Z}$ as a function of α. Neither the spheroid (oblate or prolate) nor general ellipsoid cases attain their isostatic values of $\overline{Z} = 10$ or $\overline{Z} = 12$, respectively. Reprinted with permission from A. Donev *et al.*, Phys. Rev. E **75**, 051304 (2007). Copyright 2007 American Physical Society.

the local particle arrangements are necessarily nontrivially correlated to achieve strict jamming and hence "nongeneric," the degree of which was quantified. MRJ packings of binary superdisks and of ellipses are effectively hyperuniform.[346] Note that the geometric-structure approach was used to derive a highly accurate formula for the packing fraction $\phi_{\rm MRJ}$ of MRJ binary packings of convex superdisks[187] that is valid for almost all size ratios, relative concentrations, and deformation parameter $p \geq 1/2$. For the special limit of monodisperse circular disks, this formula predicts $\phi_{\rm MRJ} = 0.837$, which is in very good agreement with the recently numerically discovered MRJ isostatic state[151] with $\phi_{\rm MRJ} = 0.827$.

3D MRJ packings of the four non-tiling Platonic solids (tetrahedra, octahedra, dodecahedra, and icosahedra) were generated using the ASC optimization scheme.[318] The MRJ packing fractions for tetrahedra, octahedra, dodecahedra, and icosahedra are 0.763 ± 0.005, 0.697 ± 0.005, 0.716 ± 0.002, and 0.707 ± 0.002, respectively. It was shown that as the number of facets of the particles increases, the translational order in the packings increases, while the orientational order decreases. Moreover, such MRJ packings were found to be hyperuniform with a total correlation function $h(\mathbf{r})$ that decays to zero asymptotically with the same power law as MRJ spheres, i.e., like $-1/r$.[4] These results suggest that hyperuniform quasi-long-range correlations are a universal feature of MRJ packings of frictionless particles of general shape. However, unlike MRJ packings of ellipsoids, superballs, and superellipsoids, which are hypostatic, MRJ packings of the non-tiling Platonic solids are isostatic.[318] In addition, 3D MRJ packings of truncated tetrahedra with an average packing fraction of 0.770 were also generated.[331]

D. Maximally dense packings

We focus here mainly on exact constructions of the densest known packings of nonspherical particles in which the lattice vectors as well as particle positions and orientations are expressible analytically. Where appropriate, we also cite some work concerning packings obtained via computer simulations and laboratory experiments.

Rigorous upper bounds on the maximal packing fraction $\phi_{\rm max}$ of packings of nonspherical particles of general shape in $\mathbb{R}^d$ can be used to assess their packing efficiency. However, it has been highly challenging to formulate upper bounds for non-tiling particle packings that are nontrivially less than unity. It has recently been shown that $\phi_{\rm max}$ of a packing of congruent nonspherical particles of volume v_P in $\mathbb{R}^d$ is bounded from the above according to

$$\phi_{\rm max} \leq \phi^U_{\rm max} = \min\left[\frac{v_P}{v_S}\,\phi^S_{\rm max}, 1\right], \tag{30}$$

where v_S is the volume of the largest sphere that can be inscribed in the nonspherical particle and $\phi^S_{\rm max}$ is the maximal packing fraction of a packing of d-dimensional of identical spheres[147,148] (e.g., $\phi^S_{\rm max} = \pi/\sqrt{12}$ for $d = 2$ and $\phi^S_{\rm max} = \pi/\sqrt{18}$ for $d = 3$). The upper bound (30) will be relatively tight provided that the *asphericity* γ (equal to the ratio of the circumradius to the inradius) of the particle is not large. Since bound (30) cannot generally be sharp (i.e., exact) for a non-tiling particle, any packing whose density is close to the upper bound (30) is nearly optimal, if not optimal. Interestingly, a majority of the centrally symmetric Platonic and Archimedean solids have relatively small asphericities, explaining the corresponding small differences between $\phi^U_{\rm max}$ and $\phi^L_{\rm max}$, the packing fraction of the densest lattice packing.[147,148,275,303] As discussed below, these densest lattice packings are conjectured to be the densest among all packings.[147,148] Upper bound (30) will also be relatively tight for superballs (superdisks) for deformation parameters p near the sphere (circle) point ($p = 1$). Dostert *et al.*[335] recently obtained upper bounds on $\phi_{\rm max}$ of *translative* packings of superballs and 3D convex bodies with tetrahedral symmetry.

1. Ellipsoids

The fact that MRJ-like packings of nearly spherical ellipsoids exist with $\phi \approx 0.74$ (see Refs. 133 and 134) suggested that there exist ordered ellipsoid packings with appreciably higher densities. The densest known packings of identical 3D ellipsoids were obtained analytically by Donev *et al.*;[305] see Fig. 15. These are exact constructions and represent a family of *non-Bravais* lattice packings of ellipsoids with a packing fraction that always exceeds that of the corresponding densest Bravais lattice packing ($\phi = 0.740\,48\ldots$) with a maximal packing fraction of $\phi = 0.7707\ldots$, for a wide range of aspect ratios ($\alpha \leq 1/\sqrt{3}$ and $\alpha \geq \sqrt{3}$). In these densest known packings, each ellipsoid has 14 contacting neighbors and there are two particles per fundamental cell.

While a convex "lens" fits snugly within an oblate spheroid of the same aspect ratio, the densest known lens packings are denser for general aspect ratios (except for a narrow range of intermediate values) than their spheroid counterparts, achieving the highest packing fraction of $\phi = \pi/4 = 0.7853\ldots$ in the "flat-lens" limit.[334]

2. Superballs

Exact analytical constructions for candidate maximally dense packings of 2D superdisks were recently proposed

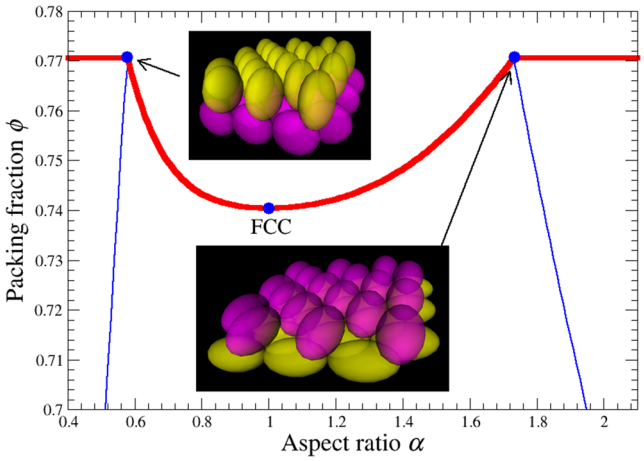

FIG. 15. The packing fraction of the "laminated" non-Bravais lattice packing of ellipsoids (with a two-particle basis) as a function of the aspect ratio α, as obtained from Ref. 305. The point $\alpha = 1$ corresponding to the face-centered cubic lattice sphere packing is shown, along with the two sharp maxima in the packing fraction for prolate ellipsoids with $\alpha = \sqrt{3}$ and oblate ellipsoids with $\alpha = 1/\sqrt{3}$, as shown in the insets. For both $\alpha < 1/\sqrt{3}$ and $\alpha > \sqrt{3}$, the packing fraction drops off precipitously holding the particle orientations fixed (blue lines). The presently maximal achievable packing fraction $\phi = 0.7707\ldots$ is highlighted with a thicker red line and is constant for $\alpha \le 1/\sqrt{3}$ and $\alpha \ge \sqrt{3}$; see Ref. 305. Reprinted with permission from A. Donev *et al.*, Phys. Rev. Lett. **92**, 255506 (2004). Copyright 2004 American Physical Society.

for all convex and concave shapes.[145] These are achieved by two different families of Bravais lattice packings such that $\phi_{\max}$ is nonanalytic at the "circular-disk" point ($p = 1$) and increases significantly as p moves away from unity. The broken rotational symmetry of superdisks influences the packing characteristics in a non-trivial way that is distinctly different from ellipse packings. For ellipse packings, no improvement over the maximal circle packing fraction ($\phi_{\max} = \pi/\sqrt{12} = 0.906\,899\ldots$) is possible, since the former is an affine transformation of the latter.[44] For superdisks, one can take advantage of the four-fold rotationally symmetric shape of the particle to obtain a substantial improvement on the maximal circle packing fraction. By contrast, one needs to use higher-dimensional counterparts of ellipses ($d \ge 3$) in order to improve on $\phi_{\max}$ for spheres. Even for 3D ellipsoids, $\phi_{\max}$ increases smoothly as the aspect ratios of the semi-axes vary from unity[305] and hence has no cusp at the sphere point. In fact, 3D ellipsoid packings have a cusp-like behavior at the sphere point only when they are randomly jammed.[133]

Jiao *et al.*[146] showed that increasing the dimensionality of a superball from two to three dimensions imbues the optimal packings with structural characteristics that are richer than their 2D counterparts. They obtained analytical constructions for the densest known superball packings for all convex and concave cases, which are certain families of Bravais lattice packings in which each particle has 12 contacting neighbors. For superballs in the cubic regime ($p > 1$), the candidate optimal packings are achieved by two families of Bravais lattice packings ($\mathbb{C}_0$ and $\mathbb{C}_1$ lattices) possessing two-fold and three-fold rotational symmetry, respectively. For superballs in the octahedral regime ($0.5 < p < 1$), there are also two families of Bravais lattices ($\mathbb{O}_0$ and $\mathbb{O}_1$ lattices) obtainable from continuous deformations of the fcc lattice, which are apparently optimal in the vicinity of the sphere point and the octahedron point, respectively.

The exact maximal packing fraction $\phi_{\max}$ as a function of deformation parameter p for convex superballs ($p \ge 1/2$) is plotted in Fig. 16. As p increases from unity, the initial increase in $\phi_{\max}$ is linear in $(p - 1)$ and subsequently $\phi_{\max}$ increases monotonically with p until it reaches unity as the particle shape tends to the cube. These characteristics stand in contrast to those of the densest known ellipsoid packings (see Fig. 15) whose packing fraction as a function of aspect ratios has zero initial slope and is bounded from the above by a value of $0.7707\ldots$.[305] As p decreases from unity, the initial increase of $\phi_{\max}$ is linear in $(1 - p)$. Thus, $\phi_{\max}$ is a nonanalytic function of p at $p = 1$.[145,146] However, the behavior of $\phi_{\max}$ as the superball shape moves off the sphere point is distinctly different from that of optimal spheroid packings, for which $\phi_{\max}$ increases smoothly as the aspect ratios of the semi-axes vary from unity and hence has no cusp at the sphere point.[305] These distinctions between the superball versus ellipsoid packings result from differences in which rotational symmetries in these two packings are broken.[146] For the small range $0.792\,48 < p < 1$, Ni *et al.*[326] numerically found lattice packings that are very slightly denser than those of the theoretically predicted $\mathbb{O}_0$ lattices of Ref. 146. Figure 17 plots the packing fraction versus deformation parameter for concave superballs ($p < 1/2$), as obtained in Ref. 146. All of these results for convex superballs support the Torquato-Jiao conjecture that the densest packings of all convex superballs are their densest lattice packings.[148]

3. Spherocylinders

The role of curvature in determining dense packings of smoothly shaped particles is still not very well understood. While the densest packings of 3D ellipsoids are (non-Bravais) lattice packings,[305] the densest packings of superballs appear to be lattice packings.[146,147] For 3D spherocylinders with $L > 0$, the optimal Bravais-lattice packing is very dense and might be one of the actual densest packings. This is

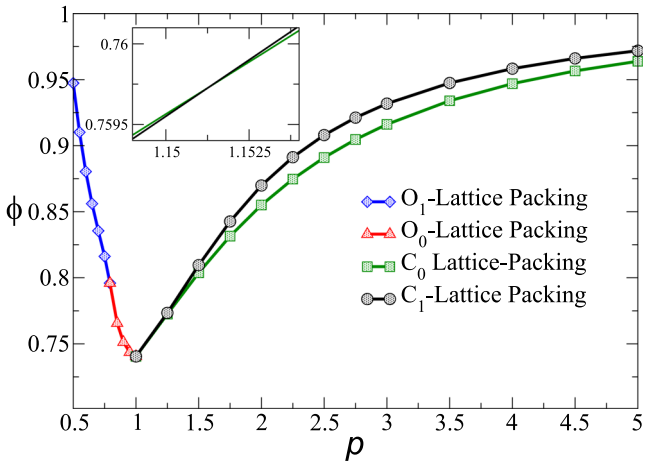

FIG. 16. Packing fraction versus deformation parameter p for the packings of convex superballs, as taken from Ref. 146. Inset: Around $p_c^* = 1.1509\ldots$, the two curves are almost locally parallel to each other. Reprinted with permission from Y. Jiao *et al.*, Phys. Rev. E **79**, 041309 (2009). Copyright 2009 American Physical Society.

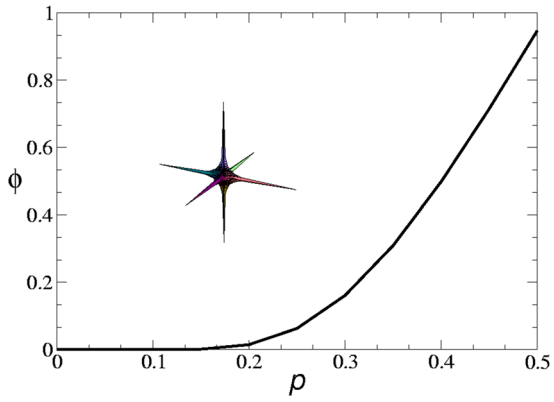

FIG. 17. Packing fraction versus deformation parameter p for the lattice packings of concave superballs, as taken from Ref. 146. Inset: a concave superball with $p = 0.1$, which will becomes a 3D cross at the limit $p \to 0$. Reprinted with permission from Y. Jiao *et al.*, Phys. Rev. E **79**, 041309 (2009). Copyright 2009 American Physical Society.

because the local principal curvature of the cylindrical surface is zero along the spherocylinder axis (i.e., a "flat" direction), and thus, spherocylinders can have very dense lattice packings by an appropriate alignment of the spherocylinders along their axes. The packing fraction of the densest Bravais lattice packing is given by

$$\phi = \frac{\pi}{\sqrt{12}} \frac{L + \frac{4}{3}R}{L + \frac{2\sqrt{6}}{3}R}, \tag{31}$$

where L is the length of the cylinder and R is the radius of the spherical caps. This lattice packing corresponds to stacking layers of aligned spherocylinders in the same manner as fcc spheres and hence there are a uncountably infinite number of non-Bravais-lattice packings of spherocylinders (in correspondence to the Barlow stackings of spheres[44]) with the same packing densities (31). Thus, the set of dense nonlattice packings of spherocylinders is overwhelmingly larger than that of the lattice packing. We will see that these dense packings are consistent with Conjecture 3 described in Sec. V D 5.

4. Polyhedra

About a decade ago, very little was known about the densest packings of polyhedral particles. The difficulty in obtaining dense packings of polyhedra is related to their complex rotational degrees of freedom and to the non-smooth nature of their shapes. It was the investigation of Conway and Torquato of dense packings of tetrahedra[307] that spurred the flurry of activity over several years to find the densest packings of tetrahedra,[147,148,310,312–315,347] which in turn led to studies of the densest packings of other polyhedra and many other nonspherical convex and concave particles.[317,321,323,324,329,334]

Torquato and Jiao[147,148] employed a Monte Carlo implementation of the ASC optimization scheme to determine dense packings of the non-tiling Platonic solids and of all of the Archimedean solids. For example, they were able to find the densest known packings of the octahedra, dodecahedra, and icosahedra (three non-tiling Platonic solids with central symmetry) with densities 0.947. . ., 0.904. . ., and 0.836. . ., respectively. Unlike the densest tetrahedron packing, which must be a non-Bravais lattice packing, the densest packings of the other non-tiling Platonic solids found by the algorithm are their previously known densest (Bravais) lattice packings;[275,303] see Fig. 18. These simulation results as well as other theoretical considerations led them to general organizing principles concerning the densest packings of a class of nonspherical particles, which are described in Sec. V D 5.

We note that the "floppy-box" (FB) method[243] is similar in spirit to the Monte Carlo implementation of the ASC method in that they both allow the periodic simulation box to change shape and size via MC moves. However, the two methods implement the box deformation differently. In the FB method, each lattice vector defining the box can be independently perturbed, implying that jamming cannot be ensured. In the ASC method, the box deformation is achieved by applying a symmetric strain tensor, which (under non-volume-increasing strains) ensures jamming in the final state. Moreover, the FB method has been used to predict crystal structures at zero and positive temperatures for systems with *hard or soft* interactions,[243,348] while the ASC method has been employed to generate jammed *ordered or disordered* hard-particle packings.[147–149,153,156,318]

Conway and Torquato[307] showed that the maximally dense packing of regular tetrahedra cannot be a Bravais lattice. Among other non-Bravais lattice packings, they obtained a simple *uniform* packing of "dimers" (two particles per fundamental cell) with packing fraction $\phi = 2/3$. A *uniform* packing has a symmetry (in this case a point inversion symmetry) that takes one tetrahedron to another. A *dimer* is composed of a pair of regular tetrahedra that exactly share a common face. They also found non-Bravais lattice (periodic) packings of regular tetrahedra with $\phi \approx 0.72$, which doubled the density of the corresponding densest Bravais-lattice packing ($\phi = 18/49 = 0.367\ldots$), which was the record before 2006. This work spurred many studies that improved on this density.[147,148,310,312–315,347] Kallus *et al.*[313] found a remarkably simple "uniform" packing of tetrahedra with high symmetry consisting of only four particles per fundamental cell (two "dimers") with packing fraction $\phi = 100/117 = 0.854\,700\ldots$. Torquato and Jiao[347] subsequently presented an analytical formulation to construct a three-parameter family of dense uniform dimer packings of tetrahedra again with four particles per fundamental cell. Making an assumption about one of these parameters resulted in a two-parameter family, including those with a packing fraction as high as $\phi = 12\,250/14\,319 = 0.855\,506\ldots$. Chen *et al.*[314] used the full three-parameter family to obtain the densest known dimer packings of tetrahedra with the very slightly higher packing fraction $\phi = 4000/4671 = 0.856\,347\ldots$ (see Fig. 19). Whether this is the optimal packing is an open question for reasons given by Torquato and Jiao.[312] The fact that the first nontrivial upper bound on the maximal packing fraction is infinitesimally smaller that unity[272] ($\phi_{\max} \leq 1 - 2.6 \times 10^{-25}$) is a testament to the difficulty in accounting for the orientations of the tetrahedra in a dense packing.

5. Organizing principles for convex and concave particles

Torquato and Jiao[147,148] showed that substantial face-to-face contacts between any of the centrally symmetric Platonic

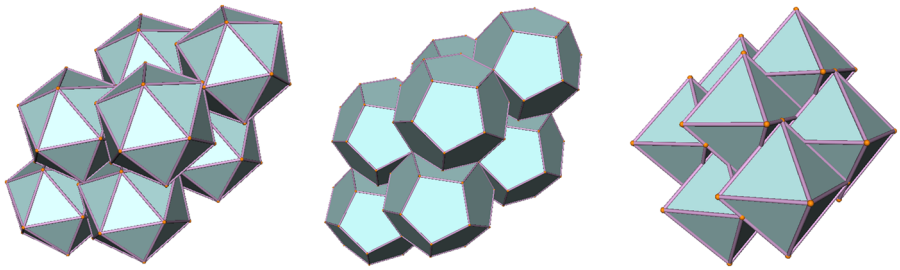

FIG. 18. Portions of the densest lattice packings of three of the centrally symmetric Platonic solids found by the ASC optimization scheme,[147,148] as taken from Ref. 148. Left panel: Icosahedron packing with packing fraction $\phi = 0.8363\ldots$. Middle panel: Dodecahedron packing with packing fraction $\phi = 0.9045\ldots$. Right panel: Octahedron packing with packing fraction $\phi = 0.9473\ldots$. Reprinted with permission from S. Torquato and Y. Jiao, Phys. Rev. E **80**, 041104 (2009). Copyright 2009 American Physical Society.

and Archimedean solids allow for a higher packing fraction. They also demonstrated that central symmetry enables maximal face-to-face contacts when particles are *aligned*, which is consistent with the densest packing being the *optimal lattice packing*. The aforementioned simulation results, upper bound, and theoretical considerations led to three conjectures concerning the densest packings of polyhedra and other nonspherical particles in $\mathbb{R}^3$; see Refs. 147, 148, and 312.

Conjecture 1. The densest packings of the centrally symmetric Platonic and Archimedean solids are given by their corresponding optimal (Bravais) lattice packings.

Conjecture 2. The densest packing of any convex congruent polyhedron without central symmetry generally is not a (Bravais) lattice packing; i.e., the set of such polyhedra whose optimal packing is not a lattice is overwhelmingly larger than the set whose optimal packing is a lattice.

Conjecture 3. The densest packings of congruent centrally symmetric particles that do not possess three equivalent principle axes (e.g., ellipsoids) are generally not (Bravais) lattice packings.

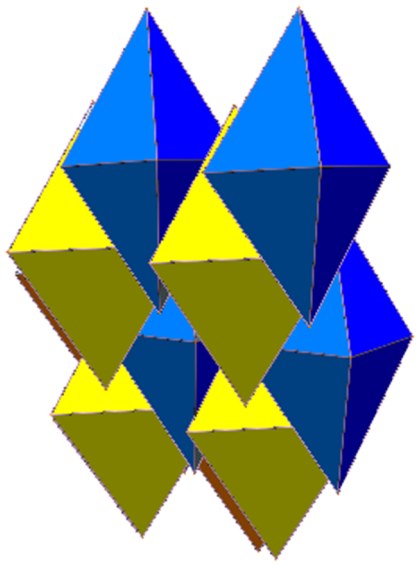

FIG. 19. A portion of the densest three-parameter family of tetrahedron packings with 4 particles per fundamental cell[321] and packing fraction $\phi = \frac{4000}{4671} = 0.856\,347\ldots$ obtained by Chen *et al.*; see Ref. 312 for a general treatment. Reprinted with permission from S. Torquato and Y. Jiao, Phys. Rev. E **86**, 011102 (2012). Copyright 2012 American Physical Society.

Conjecture 1 is the analog of Kepler's sphere conjecture for the centrally symmetric Platonic and Archimedean solids. On the experimental side, it has been shown[322] that such silver polyhedral nanoparticles self-assemble into the conjectured densest lattice packings of such shapes. Torquato and Jiao[148] have also commented on the validity of Conjecture 1 to polytopes in four and higher dimensions. The arguments leading to Conjecture 1 also strongly suggest that the densest packings of superballs and other smoothly shaped centrally symmetric convex particles having surfaces without "flat" directions are given by their corresponding optimal lattice packings.[148] Consistent with Conjecture 2, the densest known packing of the non-centrally symmetric truncated tetrahedron is a non-lattice packing with packing fraction $\phi = 207/208 = 0.995\,192\ldots$, which is amazingly close to unity and strongly implies its optimality.[317] We note that non-Bravais-lattice packings of elliptical cylinders (i.e., cylinders with an elliptical basal face) that are denser than the corresponding optimal lattice packings for any aspect ratio greater than unity have been constructed,[301,349] which is consistent with Conjecture 3. A corollary to Conjecture 3 is that the densest packings of congruent centrally symmetric particles that possess three equivalent principle axes (e.g., superballs) are generally Bravais lattices.[146]

Subsequently, Torquato and Jiao[321] generalized the aforementioned three conjectures in order to guide one to ascertain the densest packings of other convex nonspherical particles as well as *concave* shapes. These generalized organizing principles are explicitly stated as the following four distinct propositions:

Proposition 1. Dense packings of centrally symmetric convex congruent particles with three equivalent axes are given by their corresponding densest lattice packings, providing a tight density lower bound that may be optimal.

Proposition 2. Dense packings of convex congruent polyhedra without central symmetry are composed of centrally symmetric compound units of the polyhedra with the inversion-symmetric points lying on the densest lattice associated with the compound units, providing a tight density lower bound that may be optimal.

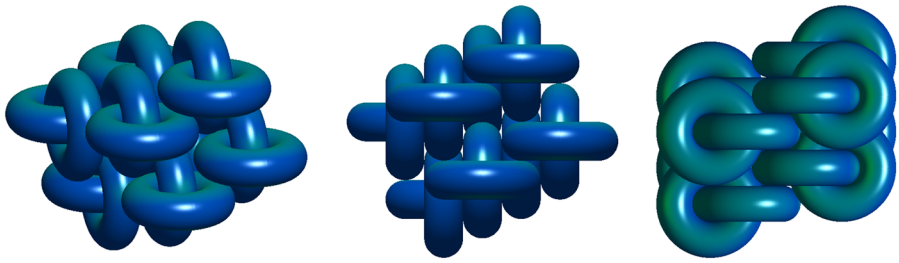

FIG. 20. The densest known packing of tori of radii ratio 2 with a packing fraction $\phi \simeq 0.7445$, as taken from Ref. 330. The images show four periodic units viewed from different angles, each containing four tori. Reprinted with permission from R. Gabbrielli *et al.*, Phys. Rev. E **89**, 022133 (2014). Copyright 2014 American Physical Society.

Proposition 3. Dense packings of centrally symmetric concave congruent polyhedra are given by their corresponding densest lattice packings, providing a tight density lower bound that may be optimal.

Proposition 4. Dense packings of concave congruent polyhedra without central symmetry are composed of centrally symmetric compound units of the polyhedra with the inversion-symmetric points lying on the densest lattice associated with the compound units, providing a tight density lower bound that may be optimal.

Proposition 1 originally concerned polyhedra. It is generalized here to include any centrally symmetric convex congruent particle with three equivalent axes to reflect the arguments put forth by Torquato and Jiao.[147,321]

All of the aforementioned organizing principles in the form of conjectures and propositions have been tested in Ref. 321 against a comprehensive set of both convex and concave particle shapes, including but not limited to the Platonic and Archimedean solids,[24,147,317] Catalan solids,[350] prisms and antiprisms,[350] Johnson solids,[350] cylinders,[301,349] lenses,[334] truncated cubes,[329] and various concave polyhedra.[350] These general organizing principles also enable one to construct analytically the densest known packings of certain convex nonspherical particles, including spherocylinders, and square pyramids and rhombic pyramids.[321] Moreover, it was shown how to apply these principles to infer the high-density equilibrium crystalline phases of hard convex and concave particles.[321] We note that the densest known 2D packings of a large family of 2D convex and concave particles (e.g., crosses, curved triangles, and moon-like shapes) fully adhere to the aforementioned organizing principles.[325]

Interestingly, the densest known packing of any identical 3D convex particle studied to date has a density that exceeds that of the optimal sphere packing value $\phi^S_{max} = \pi/\sqrt{18} = 0.7408\ldots$. These results are consistent with a conjecture of Ulam, who proposed to Gardner,[351] without any justification, that the optimal packing fraction for congruent sphere packings is smaller than that for any other convex body. There is currently no proof of Ulam's conjecture.

6. Dense packings of tori

We have seen that the preponderance of studies of dense packings of nonspherical shapes in $\mathbb{R}^3$ have dealt with convex bodies that are simply connected and thus topologically equivalent to a sphere. However, much less is known about dense packings of multiply connected solid bodies. Gabbrielli *et al.*[330] investigated the packing behavior of congruent *ring* tori in $\mathbb{R}^3$, which are multiply connected non-convex bodies of genus one, as well as *horn* and *spindle* tori. Guided by the aforementioned organizing principles, they analytically constructed a family of dense periodic packings of individual tori and found that the horn tori as well as certain spindle and ring tori can achieve a packing density not only higher than that of spheres (i.e., $\pi/\sqrt{18} = 0.7404\ldots$) but also higher than the densest known ellipsoid packings (i.e., $0.7707\ldots$). Moreover, they studied dense packings of clusters of *pair-linked* ring tori (i.e., Hopf links), which can possess much higher densities than the corresponding packings consisting of unlinked tori; see Fig. 20 for a specific example.

VI. CHALLENGES AND OPEN QUESTIONS

Packing problems are fundamental and their solutions are often profound. This perspective provides only a glimpse into the richness of packing models and their capacity to capture the salient structural and physical properties of a wide class of equilibrium and nonequilibrium condensed phases of matter that arise across the physical, mathematical, and biological sciences as well as technological applications.

Not surprisingly, there are many challenges and open questions. Is it possible to prove a first-order freezing transition in 3D hard-sphere systems? Is the fcc lattice provably the entropically favored state as the maximal density is approached along the stable crystal branch in this same system? Can one devise numerical algorithms that produced large disordered strictly jammed isostatic sphere packings that are rattler-free? Is the true MRJ state rattler-free in the thermodynamic limit? Can one prove the Torquato-Stillinger conjecture that links strictly jammed sphere packings to hyperuniformity? Can one identify incisive order metrics for packings of nonspherical particles as well as a wide class of many-particle systems that arise in molecular, biological, cosmological, and ecological systems? What are the appropriate generalizations of the jamming categories for packings of nonspherical particles? Is it possible to prove that the densest packings of the centrally symmetric Platonic and Archimedean solids are given by their corresponding optimal lattice packings? Upon extending the geometric-structure approach to Euclidean space dimensions greater than three, do periodic packings with arbitrarily large unit cells or even disordered jammed packings ever provide the highest attainable densities? Can one formulate a disordered sphere-packing model in $\mathbb{R}^d$ that can be rigorously shown to have a packing fraction that exceeds $\phi = 1/2^d$, the maximal

value achievable by the ghost RSA packing? In view of the wide interest in packing problems across the sciences, it seems reasonable to expect that substantial conceptual advances are forthcoming.

ACKNOWLEDGMENTS

I am deeply grateful to Frank Stillinger, Paul Chaikin, Aleksandar Donev, Obioma Uche, Antonello Scardicchio, Weining Man, Yang Jiao, Chase Zachary, Adam Hopkins, Étienne Marcotte, Joseph Corbo, Steven Atkinson, Remi Dreyfus, Arjun Yodh, Ge Zhang, Duyu Chen, Jianxiang Tian, Michael Klatt, Enrqiue Lomba, and Jean-Jacques Weis with whom I have collaborated on topics described in this review article. I am very thankful to Jaeuk Kim, Duyu Chen, Zheng Ma, Yang Jiao, Ge Zhang, and Gerardo Odriozola for comments that have greatly improved this article. The author's work on packing models over the years has been supported by various grants from the National Science Foundation, including the current Award No. DMR-1714722.

[1]J. E. Mayer and M. G. Mayer, *Statistical Mechanics* (John Wiley and Sons, New York, 1940).
[2]J. Percus and G. J. Yevick, "Analysis of statistical mechanics by means of collective coordinates," Phys. Rev. **110**, 1–13 (1958).
[3]J. D. Bernal, "Geometry and the structure of monatomic liquids," Nature **185**, 68–70 (1960).
[4]J. D. Bernal and J. Mason, "Packing of spheres: Co-ordination of randomly packed spheres," Nature **188**, 910 (1960).
[5]J. D. Bernal, "The geometry of the structure of liquids," in *Liquids: Structure, Properties, Solid Interactions*, edited by T. J. Hughel (Elsevier, New York, 1965), pp. 25–50.
[6]F. H. Stillinger, E. A. DiMarzio, and R. L. Kornegay, "Systematic approach to explanation of the rigid-disk phase transition," J. Chem. Phys. **40**, 1564–1576 (1964).
[7]F. Lado, "Equation of state of the hard-disk fluid from approximate integral equations," J. Chem. Phys. **49**, 3092–3096 (1968).
[8]F. H. Stillinger and Z. W. Salsburg, "Limiting polytope geometry for rigid rods, disks, and spheres," J. Stat. Phys. **1**, 179–225 (1969).
[9]J. D. Weeks, D. Chandler, and H. C. Andersen, "Role of repulsive forces in determining the equilibrium structure of simple liquids," J. Chem. Phys. **54**, 5237–5247 (1971).
[10]N. W. Ashcroft and D. N. Mermin, *Solid State Physics* (Thomson Learning, Toronto, 1976).
[11]L. V. Woodcock and C. A. Angell, "Diffusivity of the hard-sphere model in the region of fluid metastability," Phys. Rev. Lett. **47**, 1129–1132 (1981).
[12]J. P. Hansen and I. R. McDonald, *Theory of Simple Liquids* (Academic Press, New York, 1986).
[13]R. J. Speedy, "On the reproducibility of glasses," J. Chem. Phys. **100**, 6684–6691 (1994).
[14]M. Dijkstra and D. Frenkel, "Evidence for entropy-driven demixing in hard-core fluids," Phys. Rev. Lett. **72**, 298 (1994).
[15]P. M. Chaikin and T. C. Lubensky, *Principles of Condensed Matter Physics* (Cambridge University Press, New York, 1995).
[16]M. D. Rintoul and S. Torquato, "Metastability and crystallization in hard-sphere systems," Phys. Rev. Lett. **77**, 4198–4201 (1996).
[17]T. M. Truskett, S. Torquato, S. Sastry, P. G. Debenedetti, and F. H. Stillinger, "A structural precursor to freezing in the hard-disk and hard-sphere systems," Phys. Rev. E **58**, 3083 (1998).
[18]E. P. Bernard and W. Krauth, "Two-step melting in two dimensions: First-order liquid-hexatic transition," Phys. Rev. Lett. **107**, 155704 (2011).
[19]B. U. Felderhof, "Bounds for the effective dielectric constant of a suspension of uniform spheres," J. Phys. C: Solid State Phys. **15**, 3953–3966 (1982).
[20]S. Torquato, *Random Heterogeneous Materials: Microstructure and Macroscopic Properties* (Springer-Verlag, New York, 2002).
[21]T. Zohdi, "On the optical thickness of disordered particulate media," Mech. Mater. **38**, 969–981 (2006).
[22]H. Liasneuski, D. Hlushkou, S. Khirevich, A. Höltzel, U. Tallarek, and S. Torquato, "Impact of microstructure on the effective diffusivity in random packings of hard spheres," J. Appl. Phys. **116**, 034904 (2014).
[23]W. B. Russel, D. A. Saville, and W. R. Schowalter, *Colloidal Dispersions* (Cambridge University Press, Cambridge, England, 1989).
[24]S. Torquato, "Inverse optimization techniques for targeted self-assembly," Soft Matter **5**, 1157–1173 (2009).
[25]I. C. Kim and S. Torquato, "Effective conductivity of suspensions of hard spheres by Brownian motion simulation," J. Appl. Phys. **69**, 2280–2289 (1991).
[26]J. Spangenberg, G. W. Scherer, A. B. Hopkins, and S. Torquato, "Viscosity of bimodal suspensions with hard spherical particles," J. Appl. Phys. **116**, 184902 (2014).
[27]S. F. Edwards, "The role of entropy in the specification of a powder," in *Granular Matter*, edited by A. Mehta (Springer-Verlag, New York, 1994), pp. 121–140.
[28]T. Zohdi, "A computational framework for agglomeration in thermo-chemically reacting granular flows," Proc. R. Soc. London, Ser. A **460**, 3421–3445 (2004).
[29]T. Cremer and C. Cremer, "Chromosome territories, nuclear architecture and gene regulation in mammalian cells," Nat. Rev. Genet. **2**, 292 (2001).
[30]R. J. Ellis, "Macromolecular crowding: Obvious but underappreciated," Trends Biochem. Sci. **26**, 597–604 (2001).
[31]J. L. Gevertz and S. Torquato, "A novel three-phase model of brain tissue microstructure," PLoS Comput. Biol. **4**, e100052 (2008).
[32]Y. Jiao, T. Lau, H. Hatzikirou, M. Meyer-Hermann, J. C. Corbo, and S. Torquato, "Avian photoreceptor patterns represent a disordered hyperuniform solution to a multiscale packing problem," Phys. Rev. E **89**, 022721 (2014).
[33]D. Chen, W.-Y. Aw, D. Devenport, and S. Torquato, "Structural characterization and statistical-mechanical model of epidermal patterns," Biophys. J. **111**, 2534–2545 (2016).
[34]P. Prusinkiewicz and A. Lindenmayer, *The Algorithmic Beauty of Plants* (Springer-Verlag, New York, 1990).
[35]C. Nisoli, N. M. Gabor, P. E. Lammert, J. D. Maynard, and V. H. Crespi, "Annealing a magnetic cactus into phyllotaxis," Phys. Rev. E **81**, 046107 (2010).
[36]M. Tanemura and M. Hasegawa, "Geometrical models for territory. I. Models for synchronous and asynchronous settlement of territories," J. Theor. Biol. **82**, 477–496 (1980).
[37]J. H. Conway and N. J. A. Sloane, *Sphere Packings, Lattices, and Groups* (Springer-Verlag, New York, 1998).
[38]H. Cohn and N. Elkies, "New upper bounds on sphere packings. I," Ann. Math. **157**, 689–714 (2003).
[39]C. A. Rogers, *Packing and Covering* (Cambridge University Press, Cambridge, 1964).
[40]C. E. Shannon, "A mathematical theory of communication," Bell Syst. Tech. J. **27**, 379–423 (1948); "A mathematical theory of communication," **27**, 623–656 (1948).
[41]H. Cohn and A. Kumar, "Universally optimal distribution of points on spheres," J. Am. Math. Soc. **20**, 99–148 (2007).
[42]C. F. Gauss, "Besprechung des Buchs von L. A. Seeber: Untersuchungen über die Eigenschaften der positiven ternären quadratischen formen," Göttingsche Gelehrte Anzeigen **2**, 188–196 (1876); see also J. Reine Angew. Math. **1840**(20), 312–320.
[43]T. C. Hales, "A proof of the Kepler conjecture," Ann. Math. **162**, 1065–1185 (2005).
[44]S. Torquato and F. H. Stillinger, "Jammed hard-particle packings: From Kepler to Bernal and beyond," Rev. Mod. Phys. **82**, 2633 (2010).
[45]L. Onsager, "Crystal statistics. I. A two-dimensional model with an order-disorder transition," Phys. Rev. **65**, 117–149 (1944).
[46]C. Domb, "On the theory of cooperative phenomena in crystals," Adv. Phys. **9**, 149–361 (1960).
[47]G. Gallavotti, *Statistical Mechanics* (Springer-Verlag, New York, 1999).
[48]S. Torquato, "Mean nearest-neighbor distance in random packings of hard *d*-dimensional spheres," Phys. Rev. Lett. **74**, 2156–2159 (1995).
[49]S. Torquato, T. M. Truskett, and P. G. Debenedetti, "Is random close packing of spheres well defined?," Phys. Rev. Lett. **84**, 2064–2067 (2000).
[50]C. S. O'Hern, S. A. Langer, A. J. Liu, and S. R. Nagel, "Random packings of frictionless particles," Phys. Rev. Lett. **88**, 075507 (2002).
[51]C. S. O'Hern, L. E. Silbert, A. J. Liu, and S. R. Nagel, "Jamming at zero temperature and zero applied stress: The epitome of disorder," Phys. Rev. E **68**, 011306 (2003).

[52]G. Parisi and F. Zamponi, "Mean field theory of hard sphere glasses and jamming," Rev. Mod. Phys. **82**, 789–845 (2010).
[53]H. M. Jaeger, "Celebrating soft matter's 10th anniversary: Toward jamming by design," Soft Matter **11**, 12–27 (2015).
[54]J. Martinet, *Perfect Lattices in Euclidean Spaces* (Springer-Verlag, Berlin, 2003).
[55]H. Cohn, Y. Jiao, A. Kumar, and S. Torquato, "Rigidity of spherical codes," Geom. Topol. **15**, 2235–2273 (2011).
[56]S. Torquato and F. H. Stillinger, "Toward the jamming threshold of sphere packings: Tunneled crystals," J. Appl. Phys. **102**, 093511 (2007); Erratum, **103**, 129902 (2008).
[57]F. H. Stillinger, "Lattice sums and their phase diagram implications for the classical Lennard-Jones model," J. Chem. Phys. **115**, 5208–5212 (2001).
[58]L. Verlet and J. J. Weis, "Perturbation theory for the thermodynamic properties of simple liquids," Mol. Phys. **24**, 1013–1024 (1972).
[59]M. A. Rutgers, J. H. Dunsmuir, J. Z. Xue, W. B. Russel, and P. M. Chaikin, "Measurement of the hard-sphere equation of state using screened charged polystyrene colloids," Phys. Rev. B **53**, 5043–5046 (1996).
[60]A. D. Dinsmore, J. C. Crocker, and A. G. Yodh, "Self-assembly of colloidal crystals," Curr. Opin. Colloid Interface Sci. **3**, 5–11 (1998).
[61]M. Dijkstra, R. van Roij, and R. Evans, "Direct simulation of the phase behavior of binary hard-sphere mixtures: Test of the depletion potential description," Phys. Rev. Lett. **82**, 117–120 (1999).
[62]M. Dijkstra, "Entropy-driven phase transitions in colloids: From spheres to anisotropic particles," Adv. Chem. Phys. **156**, 35 (2014).
[63]A. R. Kerstein, "Percolation model of polydisperse composite solid propellant combustion," Combust. Flame **69**, 95–112 (1987).
[64]A. E. Scheidegger, *The Physics of Flow through Porous Media* (University of Toronto Press, Toronto, Canada, 1974).
[65]M. N. Rahaman, *Ceramic Processing and Sintering* (Marcel Dekker, Inc., New York, 1995).
[66]R. Demchyna, S. Leoni, H. Rosner, and U. Schwarz, "High-pressure crystal chemistry of binary intermetallic compounds," Z. Kristallogr. - Cryst. Mater. **221**, 420–434 (2006).
[67]C. Cazorla, D. Errandonea, and E. Sola, "High-pressure phases, vibrational properties, and electronic structure of $Ne(He)_2$ and $Ar(He)_2$: A first-principles study," Phys. Rev. B **80**, 064105 (2009).
[68]S. Torquato and F. H. Stillinger, "New conjectural lower bounds on the optimal density of sphere packings," Exp. Math. **15**, 307–331 (2006).
[69]S. Torquato, "Hyperuniform states of matter," Phys. Rep. **745**, 1–95 (2018).
[70]A. Donev, F. H. Stillinger, and S. Torquato, "Unexpected density fluctuations in disordered jammed hard-sphere packings," Phys. Rev. Lett. **95**, 090604 (2005).
[71]S. Torquato and F. H. Stillinger, "Local density fluctuations, hyperuniform systems, and order metrics," Phys. Rev. E **68**, 041113 (2003).
[72]C. E. Zachary and S. Torquato, "Hyperuniformity in point patterns and two-phase heterogeneous media," J. Stat. Mech.: Theory Exp. **2009**, P12015.
[73]E. C. Oğuz, J. E. S. Socolar, P. J. Steinhardt, and S. Torquato, "Hyperuniformity of quasicrystals," Phys. Rev. B **95**, 054119 (2017).
[74]S. Torquato, "Disordered hyperuniform heterogeneous materials," J. Phys.: Condens. Matter **28**, 414012 (2016).
[75]P. Debye, H. R. Anderson, and H. Brumberger, "Scattering by an inhomogeneous solid. II. The correlation function and its applications," J. Appl. Phys. **28**, 679–683 (1957).
[76]L. Boltzmann, *Lectures on Gas Theory* (University of California Press, Berkeley, California, 1898), 1964 translation by S. G. Brush of the original 1898 publication.
[77]B. J. Alder and T. E. Wainwright, "Phase transition for a hard sphere system," J. Chem. Phys. **27**, 1208–1209 (1957).
[78]H. Reiss, H. L. Frisch, and J. L. Lebowitz, "Statistical mechanics of rigid spheres," J. Chem. Phys. **31**, 369–380 (1959).
[79]Z. W. Salsburg and W. W. Wood, "Equation of state of classical hard spheres at high density," J. Chem. Phys. **37**, 798–1025 (1962).
[80]D. Frenkel, "Entropy-driven phase transitions," Phys. A **263**, 26–38 (1999).
[81]S. C. Mau and D. A. Huse, "Stacking entropy of hard-sphere crystals," Phys. Rev. E **59**, 4396–4401 (1999).
[82]R. Jadrich and K. S. Schweizer, "Equilibrium theory of the hard sphere fluid and glasses in the metastable regime up to jamming. I. Thermodynamics," J. Chem. Phys. **139**, 054501 (2013).
[83]S. Torquato, "Nearest-neighbor statistics for packings of hard spheres and disks," Phys. Rev. E **51**, 3170–3182 (1995).
[84]F. Zernike and J. A. Prins, "Die Beugung von Röntgenstrahlen in Flüssigkeiten als Effekt der Molekülanordnung," Z. Phys. **41**, 184–194 (1927).
[85]L. S. Ornstein and F. Zernike, "Accidental deviations of density and opalescence at the critical point of a single substance," Proc. Acad. Sci. (Amsterdam) **17**, 793–806 (1914).
[86]G. Stell, "The Percus–Yevick equation for the radial distribution function of a fluid," Physica **29**, 517–534 (1963).
[87]G. Zhang, F. H. Stillinger, and S. Torquato, "Transport, geometrical and topological properties of stealthy disordered hyperuniform two-phase systems," J. Chem. Phys. **145**, 244109 (2016).
[88]S. Torquato, G. Zhang, and F. H. Stillinger, "Ensemble theory for stealthy hyperuniform disordered ground states," Phys. Rev. X **5**, 021020 (2015).
[89]A. Reńyi, "On a one-dimensional problem concerning random space filling," Sel. Trans. Math. Stat. Prob. **4**, 203–218 (1963).
[90]B. Widom, "Random sequential addition of hard spheres to a volume," J. Chem. Phys. **44**, 3888–3894 (1966).
[91]L. Finegold and J. T. Donnell, "Maximum density of random placing of membrane-particles," Nature **278**, 443–445 (1979).
[92]J. Feder, "Random sequential adsorption," J. Theor. Biol. **87**, 237–254 (1980).
[93]R. H. Swendsen, "Dynamics of random sequential adsorption," Phys. Rev. A **24**, 504–508 (1981).
[94]D. W. Cooper, "Random-sequential-packing simulations in three dimensions for spheres," Phys. Rev. A **38**, 522–524 (1988).
[95]J. Talbot, P. Schaaf, and G. Tarjus, "Random sequential addition of hard spheres," Mol. Phys. **72**, 1397–1406 (1991).
[96]S. Torquato, O. U. Uche, and F. H. Stillinger, "Random sequential addition of hard spheres in high Euclidean dimensions," Phys. Rev. E **74**, 061308 (2006).
[97]G. Zhang and S. Torquato, "Precise algorithm to generate random sequential addition of hard hyperspheres at saturation," Phys. Rev. E **88**, 053312 (2013).
[98]P. J. Flory, "Intramolecular reaction between neighboring substituents of vinyl polymers," J. Am. Chem. Soc. **61**, 1518–1521 (1939).
[99]E. Roman and N. Majlis, "Computer simulation model of the structure of ion implanted impurities in semiconductors," Solid State Commun. **47**, 259–261 (1983).
[100]B. Bonnier, D. Boyer, and P. Viot, "Pair correlation function in random sequential adsorption processes," J. Phys. A: Math. Gen. **27**, 3671–3682 (1994).
[101]Z. Adamczyk, B. Siwek, M. Zembala, and P. Weroński, "Influence of polydispersity on random sequential adsorption of spherical particles," J. Colloid Interface Sci. **185**, 236–244 (1997).
[102]B. J. Brosilow, R. M. Ziff, and R. D. Vigil, "Random sequential adsorption of parallel squares," Phys. Rev. A **43**, 631–638 (1991).
[103]P. Viot, G. Tarjus, S. M. Ricci, and J. Talbot, "Random sequential adsorption of anisotropic particles: I. Jamming limit and asymptotic behavior," J. Chem. Phys. **97**, 5212–5218 (1992).
[104]R. D. Vigil and R. M. Ziff, "Random sequential adsorption of unoriented rectangles onto a plane," J. Chem. Phys. **91**, 2599–2602 (1989).
[105]O. Gromenko and V. Privman, "Random sequential adsorption of oriented superdisks," Phys. Rev. E **79**, 042103 (2009).
[106]M. Cieśla and J. Barbasz, "Random packing of regular polygons and star polygons on a flat two-dimensional surface," Phys. Rev. E **90**, 022402 (2014).
[107]G. Zhang, "Precise algorithm to generate random sequential adsorption of hard polygons at saturation," Phys. Rev. E **97**, 043311 (2018).
[108]J. D. Sherwood, "Packing of spheroids in three-dimensional space by random sequential addition," J. Phys. A: Math. Gen. **30**, L839 (1997).
[109]B. Bonnier, "On the random sequential adsorption of d-dimensional cubes," J. Phys. A: Math. Gen. **34**, 10757–10762 (2001).
[110]M. Cieśla and P. Kubala, "Random sequential adsorption of cubes," J. Chem. Phys. **148**, 024501 (2018).
[111]S. Torquato and F. H. Stillinger, "Exactly solvable disordered sphere-packing model in arbitrary-dimensional Euclidean spaces," Phys. Rev. E **73**, 031106 (2006).
[112]G. D. Scott and D. M. Kilgour, "The density of random close packing of spheres," Brit. J. Appl. Phys. **2**, 863–866 (1969).
[113]Anonymous, "What is random packing?," Nature **239**, 488–489 (1972).
[114]K. Gotoh and J. L. Finney, "Statistical geometrical approach to random packing density of equal spheres," Nature **252**, 202–205 (1974).

[115]J. G. Berryman, "Random close packing of hard spheres and disks," Phys. Rev. A **27**, 1053–1061 (1983).
[116]W. S. Jodrey and E. M. Tory, "Computer simulation of close random packing of equal spheres," Phys. Rev. A **32**, 2347–2351 (1985).
[117]A. Z. Zinchenko, "Algorithm for random close packing of spheres with periodic boundary conditions," J. Comput. Phys. **114**, 298–307 (1994).
[118]R. Jullien, J.-F. Sadoc, and R. Mosseri, "Packing at random in curved space and frustration: A numerical study," J. Phys. I **7**, 1677–1692 (1997).
[119]O. Pouliquen, M. Nicolas, and P. D. Weidman, "Crystallization of non-Brownian spheres under horizontal shaking," Phys. Rev. Lett. **79**, 3640–3643 (1997).
[120]B. D. Lubachevsky and F. H. Stillinger, "Geometric properties of random disk packings," J. Stat. Phys. **60**, 561–583 (1990).
[121]A. Donev, S. Torquato, F. H. Stillinger, and R. Connelly, "Jamming in hard sphere and disk packings," J. Appl. Phys. **95**, 989–999 (2004).
[122]S. F. Edwards and D. V. Grinev, "The tensorial formulation of volume function for packings of particles," Chem. Eng. Sci. **56**, 5451–5455 (2001).
[123]A. J. Liu and S. R. Nagel, "Jamming is not just cool anymore," Nature **396**, 21–22 (1998).
[124]H. A. Makse and J. Kurchan, "Testing the thermodynamic approach to granular matter with a numerical model of a decisive experiment," Nature **415**, 614–617 (2002).
[125]L. E. Silbert, D. Ertas, G. S. Grest, T. C. Halsey, and D. Levine, "Geometry of frictionless and frictional sphere packings," Phys. Rev. E **65**, 031304 (2002).
[126]M. Wyart, L. E. Silbert, S. R. Nagel, and T. A. Witten, "Effects of compression on the vibrational modes of marginally jammed solids," Phys. Rev. E **72**, 051306 (2005).
[127]L. E. Silbert, A. J. Liu, and S. R. Nagel, "Vibrations and diverging length scales near the unjamming transition," Phys. Rev. Lett. **95**, 098301 (2005).
[128]G.-J. Gao, J. Blawzdziewicz, and C. S. O'Hern, "Understanding the frequency distribution of mechanically stable disk packings," Phys. Rev. E **74**, 061304 (2006).
[129]C. Song, P. Wang, and H. A. Makse, "A phase diagram for jammed matter," Nature **453**, 629–632 (2008).
[130]S. Torquato and F. H. Stillinger, "Multiplicity of generation, selection, and classification procedures for jammed hard-particle packings," J. Phys. Chem. B **105**, 11849–11853 (2001).
[131]A. R. Kansal, S. Torquato, and F. H. Stillinger, "Diversity of order and densities in jammed hard-particle packings," Phys. Rev. E **66**, 041109 (2002).
[132]S. Torquato, A. Donev, and F. H. Stillinger, "Breakdown of elasticity theory for jammed hard-particle packings: Conical nonlinear constitutive theory," Int. J. Solids Struct. **40**, 7143–7153 (2003).
[133]A. Donev, I. Cisse, D. Sachs, E. A. Variano, F. H. Stillinger, R. Connelly, S. Torquato, and P. M. Chaikin, "Improving the density of jammed disordered packings using ellipsoids," Science **303**, 990–993 (2004).
[134]A. Donev, R. Connelly, F. H. Stillinger, and S. Torquato, "Underconstrained jammed packings of nonspherical hard particles: Ellipses and ellipsoids," Phys. Rev. E **75**, 051304 (2007).
[135]R. Connelly, K. Bezdek, and A. Bezdek, "Finite and uniform stability of sphere packings," Discrete Comput. Geom. **20**, 111–130 (1998).
[136]A. Donev, S. Torquato, F. H. Stillinger, and R. Connelly, "A linear programming algorithm to test for jamming in hard-sphere packings," J. Comput. Phys. **197**, 139–166 (2004).
[137]T. Aste, M. Saadatfar, and T. Senden, "Local and global relations between the number of contacts and density in monodisperse sphere packs," J. Stat. Mech. **2006**, P07010.
[138]J. Brujić, S. F. Edwards, I. Hopkinson, and H. A. Makse, "Measuring distribution of interdroplet forces in a compressed emulsion system," Phys. A **327**, 201–212 (2003).
[139]W. Man, A. Donev, F. H. Stillinger, M. Sullivan, W. B. Russel, D. Heeger, S. Inati, S. Torquato, and P. M. Chaikin, "Experiments on random packing of ellipsoids," Phys. Rev. Lett. **94**, 198001 (2005).
[140]A. Donev, S. Torquato, and F. H. Stillinger, "Pair correlation function characteristics of nearly jammed disordered and ordered hard-sphere packings," Phys. Rev. E **71**, 011105-1–011105-14 (2005).
[141]R. D. Kamien and A. J. Liu, "Why is random close packing reproducible?," Phys. Rev. Lett. **99**, 155501 (2007).
[142]T. M. Truskett, S. Torquato, and P. G. Debenedetti, "Towards a quantification of disorder in materials: Distinguishing equilibrium and glassy sphere packings," Phys. Rev. E **62**, 993–1001 (2000).
[143]A. Donev, S. Torquato, and F. H. Stillinger, "Neighbor list collision-driven molecular dynamics for nonspherical hard particles. I. Algorithmic details," J. Comput. Phys. **202**, 737–764 (2005).
[144]A. Donev, S. Torquato, and F. H. Stillinger, "Neighbor list collision-driven molecular dynamics for nonspherical hard particles. II. Applications to ellipses and ellipsoids," J. Comput. Phys. **202**, 765–793 (2005).
[145]Y. Jiao, F. H. Stillinger, and S. Torquato, "Optimal packings of superdisks and the role of symmetry," Phys. Rev. Lett. **100**, 245505 (2008).
[146]Y. Jiao, F. H. Stillinger, and S. Torquato, "Optimal packings of superballs," Phys. Rev. E **79**, 041309 (2009).
[147]S. Torquato and Y. Jiao, "Dense packings of the platonic and archimedean solids," Nature **460**, 876–881 (2009).
[148]S. Torquato and Y. Jiao, "Dense polyhedral packings: Platonic and archimedean solids," Phys. Rev. E **80**, 041104 (2009).
[149]S. Torquato and Y. Jiao, "Robust algorithm to generate a diverse class of dense disordered and ordered sphere packings via linear programming," Phys. Rev. E **82**, 061302 (2010).
[150]S. Atkinson, F. H. Stillinger, and S. Torquato, "Detailed characterization of rattlers in exactly isostatic, strictly jammed sphere packings," Phys. Rev. E **88**, 062208 (2013).
[151]S. Atkinson, F. H. Stillinger, and S. Torquato, "Existence of isostatic, maximally random jammed monodisperse hard-disk packings," Proc. Natl. Acad. Sci. U. S. A. **111**, 18436–18441 (2014).
[152]S. Atkinson, G. Zhang, A. B. Hopkins, and S. Torquato, "Critical slowing down and hyperuniformity on approach to jamming," Phys. Rev. E **94**, 012902 (2016).
[153]Y. Jiao, F. H. Stillinger, and S. Torquato, "Nonuniversality of density and disorder of jammed sphere packings," J. Appl. Phys. **109**, 013508 (2011).
[154]A. B. Hopkins, Y. Jiao, F. H. Stillinger, and S. Torquato, "Phase diagram and structural diversity of the densest binary sphere packings," Phys. Rev. Lett. **107**, 125501 (2011).
[155]A. B. Hopkins, F. H. Stillinger, and S. Torquato, "Densest binary sphere packings," Phys. Rev. E **85**, 021130 (2012).
[156]É. Marcotte and S. Torquato, "Efficient linear programming algorithm to generate the densest lattice sphere packings," Phys. Rev. E **87**, 063303 (2013).
[157]Y. Kallus, É. Marcotte, and S. Torquato, "Jammed lattice sphere packings," Phys. Rev. E **88**, 062151 (2013).
[158]M. D. Rintoul, S. Torquato, C. L. Y. Yeong, S. Erramilli, D. Keane, D. L. Dabbs, and I. A. Aksay, "Structure and transport properties of a porous magnetic gel via x-ray microtomography," Phys. Rev. E **54**, 2663–2669 (1996).
[159]J. R. Errington, P. G. Debenedetti, and S. Torquato, "Quantification of order in the Lennard-Jones system," J. Chem. Phys. **118**, 2256 (2003).
[160]G. Zhang, F. H. Stillinger, and S. Torquato, "The perfect glass paradigm: Disordered hyperuniform glasses down to absolute zero," Sci. Rep. **6**, 36963 (2016).
[161]J. R. Errington and P. G. Debenedetti, "Relationship between structural order and the anomalies of liquid water," Nature **409**, 318–321 (2001).
[162]J. R. Errington, P. G. Debenedetti, and S. Torquato, "Cooperative origin of low-density domains in liquid water," Phys. Rev. Lett. **89**, 215503 (2002).
[163]R. A. DiStasio, G. Zhang, F. H. Stillinger, and S. Torquato, "Rational design of stealthy hyperuniform patterns with tunable order," Phys. Rev. E **97**, 023311 (2018).
[164]A. R. Kansal, T. M. Truskett, and S. Torquato, "Nonequilibrium hard-disk packings with controlled orientational order," J. Chem. Phys. **113**, 4844–4851 (2000).
[165]P. J. Steinhardt, D. R. Nelson, and M. Ronchetti, "Bond-orientational order in liquids and glasses," Phys. Rev. B **28**, 784–805 (1983).
[166]Z. H. Stachurski, "Definition and properties of ideal amorphous solids," Phys. Rev. Lett. **90**, 155502 (2003).
[167]L. Fejes Tóth, *Regular Figures* (Macmillan, New York, 1964).
[168]F. J. Burnell and S. L. Sondhi, "Classical antiferromagnetism on Torquato-Stillinger packings," Phys. Rev. B **78**, 024407 (2008).
[169]R. Zallen, *The Physics of Amorphous Solids* (Wiley, New York, 1983).
[170]S. Torquato, A. Scardicchio, and C. E. Zachary, "Point processes in arbitrary dimension from Fermionic gases, random matrix theory, and number theory," J. Stat. Mech.: Theory Exp. **2008**, P11019.
[171]R. P. Feynman and M. Cohen, "Energy spectrum of the excitations in liquid helium," Phys. Rev. **102**, 1189–1204 (1956).
[172]L. Reatto and G. V. Chester, "Phonons and the properties of a Bose system," Phys. Rev. **155**, 88–100 (1967).

[173]M. Skoge, A. Donev, F. H. Stillinger, and S. Torquato, "Packing hyperspheres in high-dimensional Euclidean spaces," Phys. Rev. E **74**, 041127 (2006).
[174]A. B. Hopkins, F. H. Stillinger, and S. Torquato, "Nonequilibrium static diverging length scales on approaching a prototypical model glassy state," Phys. Rev. E **86**, 021505 (2012).
[175]S. Atkinson, F. H. Stillinger, and S. Torquato, "Static structural signatures of nearly jammed disordered and ordered hard-sphere packings: Direct correlation function," Phys. Rev. E **94**, 032902 (2016).
[176]J. Haberko, N. Muller, and F. Scheffold, "Direct laser writing of three dimensional network structures as templates for disordered photonic materials," Phys. Rev. A **88**, 043822 (2013).
[177]É. Marcotte, F. H. Stillinger, and S. Torquato, "Nonequilibrium static growing length scales in supercooled liquids on approaching the glass transition," J. Chem. Phys. **138**, 12A508 (2013).
[178]A. Ikeda and L. Berthier, "Thermal fluctuations, mechanical response, and hyperuniformity in jammed solids," Phys. Rev. E **92**, 012309 (2015).
[179]Y. Wu, P. Olsson, and S. Teitel, "Search for hyperuniformity in mechanically stable packings of frictionless disks above jamming," Phys. Rev. E **92**, 052206 (2015).
[180]A. Ikeda, L. Berthier, and G. Parisi, "Large-scale structure of randomly jammed spheres," Phys. Rev. E **95**, 052125 (2017).
[181]B. D. Lubachevsky, F. H. Stillinger, and E. N. Pinson, "Disks versus spheres: Contrasting properties of random packings," J. Stat. Phys. **64**, 501–524 (1991).
[182]M. A. Klatt and S. Torquato, "Characterization of maximally random jammed sphere packings: Voronoi correlation functions," Phys. Rev. E **90**, 052120 (2014).
[183]M. A. Klatt and S. Torquato, "Characterization of maximally random jammed sphere packings. II. Correlation functions and density fluctuations," Phys. Rev. E **94**, 022152 (2016).
[184]M. A. Klatt and S. Torquato, "Characterization of maximally random jammed sphere packings. III. Transport and electromagnetic properties via correlation functions," Phys. Rev. E **97**, 012118 (2018).
[185]M. C. Rechtsman and S. Torquato, "Effective dielectric tensor for electromagnetic wave propagation in random media," J. Appl. Phys. **103**, 084901 (2008).
[186]R. M. Ziff and S. Torquato, "Percolation of disordered jammed sphere packings," J. Phys. A: Math. Theor. **50**, 085001 (2017).
[187]J. Tian, Y. Xu, Y. Jiao, and S. Torquato, "A geometric-structure theory for maximally random jammed packings," Sci. Rep. **5**, 16722 (2015).
[188]S. I. Henderson, T. C. Mortensen, S. M. Underwood, and W. van Megen, "Effect of particle size distribution on crystallisation and the glass transition of hard sphere colloids," Phys. A **233**, 102–116 (1996).
[189]G. V. Schulz, "Über die Kinetik der Kettenpolymerisationen," Z. Phys. Chem. **B43**, 25–46 (1939).
[190]H. Cramer, *Mathematical Methods of Statistics* (Princeton University Press, Princeton, 1954).
[191]J. L. Lebowitz, "Exact solution of generalized Percus–Yevick equation for a mixture of hard spheres," Phys. Rev. **133**, A895–A899 (1964).
[192]B. Widom and J. S. Rowlinson, "New model for the study of liquid–vapor phase transitions," J. Chem. Phys. **52**, 1670–1684 (1970).
[193]J. L. Lebowitz and D. Zomick, "Mixtures of hard spheres with nonadditive diameters: Some exact results and solution of py equation," J. Chem. Phys. **54**, 3335–3346 (1971).
[194]G. A. Mansoori, N. F. Carnahan, K. E. Starling, and T. W. Leland, "Equilibrium thermodynamic properties of the mixture of hard spheres," J. Chem. Phys. **54**, 1523–1525 (1971).
[195]J. J. Salacuse and G. Stell, "Polydisperse systems: Statistical thermodynamics, with applications to several models including hard and permeable spheres," J. Chem. Phys. **77**, 3714–3725 (1982).
[196]J. H. Nixon and M. Silbert, "Percus-Yevick results for a binary mixture of hard spheres with non-additive diameters. I. Negative non-additive parameter," Mol. Phys. **52**, 207–224 (1984).
[197]Y. Rosenfeld, "Free-energy model for the inhomogeneous hard-sphere fluid mixture and density-functional theory of freezing," Phys. Rev. Lett. **63**, 980–983 (1989).
[198]W. G. T. Kranendonk and D. Frenkel, "Computer simulation of solid-liquid coexistence in binary hard sphere mixtures," Mol. Phys. **72**, 679–697 (1991).
[199]P. Bartlett, R. H. Ottewill, and P. N. Pusey, "Superlattice formation in binary mixtures of hard-sphere colloids," Phys. Rev. Lett. **68**, 3801 (1992).
[200]M. D. Eldridge, P. A. Madden, and D. Frenkel, "Entropy-driven formation of a superlattice in a hard-sphere binary mixture," Nature **365**, 35 (1993).
[201]M. D. Eldridge, P. A. Madden, P. N. Pusey, and P. Bartlett, "Binary hard-sphere mixtures: A comparison between computer simulation and experiment," Mol. Phys. **84**, 395–420 (1995).
[202]R. Dickman and G. Stell, "Critical behavior of the Widom–Rowlinson lattice model," J. Chem. Phys. **102**, 8674–8676 (1995).
[203]C.-Y. Shew and A. Yethiraj, "Phase behavior of the Widom–Rowlinson mixture," J. Chem. Phys. **104**, 7665–7670 (1996).
[204]E. Lomba, M. Alvarez, L. L. Lee, and N. G. Almarza, "Phase stability of binary non-additive hard-sphere mixtures: A self-consistent integral equation study," J. Chem. Phys. **104**, 4180–4188 (1996).
[205]T. Biben and J.-P. Hansen, "Osmotic depletion, non-additivity and phase separation," Phys. A **235**, 142–148 (1997).
[206]A. Santos, S. B. Yuste, and M. L. De Haro, "Equation of state of a multicomponent d-dimensional hard-sphere fluid," Mol. Phys. **96**, 1 (1999).
[207]M. Dijkstra, "Phase behavior of nonadditive hard-sphere mixtures," Phys. Rev. E **58**, 7523 (1998).
[208]W. T. Góźdź, "Critical-point and coexistence curve properties of a symmetric mixture of nonadditive hard spheres: A finite size scaling study," J. Chem. Phys. **119**, 3309–3315 (2003).
[209]E. Trizac, M. D. Eldridge, and P. A. Madden, "Stability of the ab crystal for asymmetric binary hard sphere mixtures," Mol. Phys. **90**, 675–678 (1997).
[210]A.-P. Hynninen, J. H. J. Thijssen, E. C. M. Vermolen, M. Dijkstra, and A. Van Blaaderen, "Self-assembly route for photonic crystals with a bandgap in the visible region," Nat. Mater. **6**, 202 (2007).
[211]A.-P. Hynninen, L. Filion, and M. Dijkstra, "Stability of LS and LS_2 crystal structures in binary mixtures of hard and charged spheres," J. Chem. Phys. **131**, 064902 (2009).
[212]R. Roth, "Fundamental measure theory for hard-sphere mixtures: A review," J. Phys.: Condens. Matter **22**, 063102 (2010).
[213]A. Santos, S. B. Yuste, M. L. de Haro, and V. Ogarko, "Equation of state of polydisperse hard-disk mixtures in the high-density regime," Phys. Rev. E **96**, 062603 (2017).
[214]F. Lado, "Integral equation theory of polydisperse colloidal suspensions using orthogonal polynomial expansions," Phys. Rev. E **54**, 4411 (1996).
[215]E. Lomba, J.-J. Weis, and S. Torquato, "Disordered hyperuniformity in two-component non-additive hard disk plasmas," Phys. Rev. E **96**, 062126 (2017).
[216]E. Lomba, J.-J. Weis, and S. Torquato, "Disordered multihyperuniformity derived from binary plasmas," Phys. Rev. E **97**, 010102(R) (2018).
[217]W. M. Visscher and M. Bolsterli, "Random packing of equal and unequal spheres in two and three dimensions," Nature **239**, 504–507 (1972).
[218]A. S. Clarke and J. D. Wiley, "Numerical simulation of a dense random packing of a binary mixture of hard spheres," Phys. Rev. B **35**, 7350–7356 (1987).
[219]A. Yang, C. T. Miller, and L. D. Turcoliver, "Simulation of correlated and uncorrelated packing of random size spheres," Phys. Rev. E **53**, 1516–1524 (1996).
[220]P. Richard, L. Oger, J. P. Troadec, and A. Gervois, "Tessellation of binary assemblies of spheres," Phys. A **259**, 205–221 (1998).
[221]E. Santiso and E. A. Müller, "Dense packing of binary and polydisperse hard spheres," Mol. Phys. **100**, 2461–2469 (2002).
[222]K. de Lange Kristiansen, A. Wouterse, and A. Philipse, "Simulation of random packing of binary sphere mixtures by mechanical contraction," Phys. A **358**, 249–262 (2005).
[223]A. R. Kansal, S. Torquato, and F. H. Stillinger, "Computer generation of dense polydisperse sphere packing," J. Chem. Phys. **117**, 8212–8218 (2002).
[224]P. Chaudhuri, L. Berthier, and S. Sastry, "Jamming transitions in amorphous packings of frictionless spheres occur over a continuous range of volume fractions," Phys. Rev. Lett. **104**, 165701 (2010).
[225]M. Clusel, E. I. Corwin, A. O. N. Siemens, and J. Brujić, "A 'granocentric' model for random packing of jammed emulsions," Nature **460**, 611–615 (2009).
[226]H. Sakai, F. H. Stillinger, and S. Torquato, "Equi-*g(r)* sequences of systems derived from the square-well potential," J. Chem. Phys. **117**, 297–307 (2002).
[227]A. B. Hopkins, F. H. Stillinger, and S. Torquato, "Disordered strictly jammed binary sphere packings attain an anomalously large range of densities," Phys. Rev. E **88**, 022205 (2013).
[228]D. Chen and S. Torquato, "Confined disordered strictly jammed binary sphere packings," Phys. Rev. E **92**, 062207 (2015).

[229]A. Donev, F. H. Stillinger, and S. Torquato, "Do binary hard disks exhibit an ideal glass transition?," Phys. Rev. Lett. **96**, 225502 (2006).
[230]A. Donev, F. H. Stillinger, and S. Torquato, "Configurational entropy of binary hard-disk glasses: Nonexistence of an ideal glass transition," J. Chem. Phys. **127**, 124509 (2007).
[231]G. Parisi and F. Zamponi, "The ideal glass transition of hard spheres," J. Chem. Phys. **123**, 144501 (2005).
[232]C. E. Zachary, Y. Jiao, and S. Torquato, "Hyperuniform long-range correlations are a signature of disordered jammed hard-particle packings," Phys. Rev. Lett. **106**, 178001 (2011).
[233]C. E. Zachary, Y. Jiao, and S. Torquato, "Hyperuniformity, quasi-long-range correlations, and void-space constraints in maximally random jammed particle packings. I. Polydisperse spheres," Phys. Rev. E **83**, 051308 (2011).
[234]L. Berthier, P. Chaudhuri, C. Coulais, O. Dauchot, and P. Sollich, "Suppressed compressibility at large scale in jammed packings of size-disperse spheres," Phys. Rev. Lett. **106**, 120601 (2011).
[235]R. Dreyfus, Y. Xu, T. Still, L. A. Hough, A. G. Yodh, and S. Torquato, "Diagnosing hyperuniformity in two-dimensional, disordered, jammed packings of soft spheres," Phys. Rev. E **91**, 012302 (2015).
[236]J. Ricouvier, R. Pierrat, R. Carminati, P. Tabeling, and P. Yazhgur, "Optimizing hyperuniformity in self-assembled bidisperse emulsions," Phys. Rev. Lett. **119**, 208001 (2017).
[237]H. J. Herrmann, G. Mantica, and D. Bessis, "Space-filling bearings," Phys. Rev. Lett. **65**, 3223–3226 (1990).
[238]C. N. Likos and C. L. Henley, "Complex alloy phases for binary hard-disk mixtures," Philos. Mag. B **68**, 85–113 (1993).
[239]O. U. Uche, F. H. Stillinger, and S. Torquato, "Concerning maximal packing arrangements of binary disk mixtures," Phys. A **342**, 428–446 (2004).
[240]A. Florian, "Ausfüllung der Ebene durch Kreise," Rend. Circ. Mat. Palermo **9**, 300–312 (1960).
[241]T. S. Hudson and P. Harrowell, "Dense packings of hard spheres of different sizes based on filling interstices in uniform three-dimensional tilings," J. Phys. Chem. B **112**, 8139–8143 (2008).
[242]J. K. Kummerfeld, T. S. Hudson, and P. Harrowell, "The densest packing of ab binary hard-sphere homogeneous compounds across all size ratios," J. Phys. Chem. B **112**, 10773–10776 (2008).
[243]L. Filion and M. Dijkstra, "Prediction of binary hard-sphere crystal structures," Phys. Rev. E **79**, 046714 (2009).
[244]J. H. Conway and N. J. A. Sloane, "What are all the best sphere packings n low dimensions?," Discrete Comput. Geom. **13**, 383–403 (1995).
[245]H. L. Frisch and J. K. Percus, "High dimensionality as an organizing device for classical fluids," Phys. Rev. E **60**, 2942–2948 (1999).
[246]G. Parisi and F. Slanina, "Toy model for the mean-field theory of hard-sphere liquids," Phys. Rev. E **62**, 6554–6559 (2000).
[247]N. D. Elkies, "Lattices, linear codes, and invariants. Part I," Not. AMS **47**, 1238–1245 (2000).
[248]G. Parisi and F. Zamponi, "Amorphous packings of hard spheres for large space dimension," J. Stat. Mech.: Theory Exp. **2006**, P03017.
[249]H. Cohn, "New upper bounds on sphere packings. II," Geom. Topol. **6**, 329–353 (2002).
[250]S. Torquato, "Necessary conditions on realizable two-point correlation functions of random media," Ind. Eng. Chem. Res. **45**, 6923–6928 (2006).
[251]D. René Rohrmann and A. Santos, "Structure of hard-hypersphere fluids in odd dimensions," Phys. Rev. E **76**, 051202 (2007).
[252]M. Adda-Bedia, E. Katzav, and D. Vella, "Solution of the percus-yevick equation for hard hyperspheres in even dimensions," J. Chem. Phys. **129**, 144506 (2008).
[253]A. Scardicchio, F. H. Stillinger, and S. Torquato, "Estimates of the optimal density of sphere packings in high dimensions," J. Math. Phys. **49**, 043301 (2008).
[254]H. Cohn and A. Kumar, "Optimality and uniqueness of the Leech lattice among lattices," Ann. Math. **170**, 1003–1050 (2009).
[255]J. A. van Meel, D. Frenkel, and P. Charbonneau, "Geometrical frustration: A study of four-dimensional hard spheres," Phys. Rev. E **79**, 030201 (2009).
[256]J. A. van Meel, B. Charbonneau, A. Fortini, and P. Charbonneau, "Hard sphere crystallization gets rarer with increasing dimension," Phys. Rev. E **80**, 061110 (2009).
[257]L. Lue, M. Bishop, and P. A. Whitlock, "The fluid to solid phase transition of hard hyperspheres in four and five dimensions," J. Chem. Phys. **132**, 104509 (2010).
[258]Y. Kallus and S. Torquato, "Marginal stability in jammed packings: Quasicontacts and weak contacts," Phys. Rev. E **90**, 022114 (2014).
[259]A. Andreanov, A. Scardicchio, and S. Torquato, "Extreme lattices: Symmetries and decorrelation," J. Stat. Mech.: Theory Exp. **2016**, 113301.
[260]L. Berthier and T. A. Witten, "Glass transition of dense fluids of hard and compressible spheres," Phys. Rev. E **80**, 021502 (2009).
[261]M. Viazovska, "The sphere packing problem in dimension 8," Ann. Math. **185**, 991–1015 (2017).
[262]H. Cohn, A. Kumar, S. D. Miller, D. Radchenko, and M. Viazovska, "The sphere packing problem in dimension 24," Ann. Math. **185**, 1017–1033 (2017).
[263]M. Luban and A. Baram, "Third and fourth virial coefficients of hard hyperspheres of arbitrary dimensionality," J. Chem. Phys. **76**, 3233–3241 (1982).
[264]N. Clisby and B. M. McCoy, "Ninth and tenth order virial coefficients for hard spheres in D dimensions," J. Stat. Phys. **122**, 15–57 (2006).
[265]R. Finken, M. Schmidt, and H. Löwen, "Freezing transition of hard hyperspheres," Phys. Rev. E **65**, 016108 (2001).
[266]S. Torquato, "Effect of dimensionality on the continuum percolation of overlapping hyperspheres and hypercubes," J. Chem. Phys. **136**, 054106 (2012).
[267]S. Torquato and F. H. Stillinger, "Controlling the short-range order and packing densities of many-particle systems," J. Phys. Chem. B **106**, 8354–8359 (2002); Erratum, **106**, 11406 (2002).
[268]Y. Jin, P. Charbonneau, S. Meyer, C. Song, and F. Zamponi, "Application of Edwards' statistical mechanics to high-dimensional jammed sphere packings," Phys. Rev. E **82**, 051126 (2010).
[269]P. Charbonneau, E. I. Corwin, G. Parisi, and F. Zamponi, "Universal microstructure and mechanical stability of jammed packings," Phys. Rev. Lett. **109**, 205501 (2012).
[270]A. Schürmann, M. D. Sikirić, and F. Vallentin, "A generalization of Voronoi's reduction theory and its application," Duke Math. J. **142**, 127–164 (2008).
[271]S. Torquato, "Reformulation of the covering and quantizer problems as ground states of interacting particles," Phys. Rev. E **82**, 056109 (2010).
[272]S. Gravel, V. Elser, and Y. Kallus, "Upper bound on the packing density of regular tetrahedra and octahedra," Discrete Comput. Geom. **46**, 799–818 (2011).
[273]A. Andreanov and A. Scardicchio, "Random perfect lattices and the sphere packing problem," Phys. Rev. E **86**, 041117 (2012).
[274]M. Ajtai, "The shortest vector problem in L_2 is np-hard for randomized reductions," in STOC '98: Proceedings of the Thirtieth Annual ACM Symposium on Theory of Computing, 1998, pp. 10–19.
[275]H. Minkowski, "Diskontinuitätsbereich für arithmetische Äquivalenz," J. Reine Angew. Math. **129**, 220–274 (1905).
[276]H. Davenport and C. Rogers, "Hlawka's theorem in the geometry of numbers," Duke J. Math. **14**, 367–375 (1947).
[277]K. Ball, "A lower bound for the optimal density of lattice packings," Int. Math. Res. Not. **1992**, 217–221.
[278]S. I. Vance, "Lattices and sphere packings in Euclidean space," Ph.D. thesis, University of Washington, 2009.
[279]H. Blichfeldt, "The minimum value of quadratic forms and the closest packing of spheres," Math. Ann. **101**, 605–608 (1929).
[280]C. A. Rogers, "The packing of equal spheres," Proc. London Math. Soc. **s3-8**, 609–620 (1958).
[281]G. A. Kabatiansky and V. I. Levenshtein, "Bounds for packings on a sphere and in space," Probl. Inf. Transm. **14**, 3–25 (1978).
[282]C. E. Zachary and S. Torquato, "High-dimensional generalizations of the kagome and diamond crystals and the decorrelation principle for periodic sphere packings," J. Stat. Mech.: Theory Exp. **2011**, P10017.
[283]J. M. Renes, "Equiangular spherical codes in quantum cryptography," Quantum Inf. Comput. **5**, 81–92 (2005).
[284]M. J. Bowick, A. Cacciuto, D. R. Nelson, and A. Travesset, "Crystalline particle packings on a sphere with long-range power-law potentials," Phys. Rev. B **73**, 024115 (2006).
[285]C. D. Modes and R. D. Kamien, "Hard discs on the hyperbolic plane," Phys. Rev. Lett. **99**, 235701 (2007).
[286]P. M. L. Tammes, "On the origin of number and arrangement of the places of exit on the surface of pollen-grains," Recueil des Tavaux Botaniques Nérlandais **27**, 1–84 (1930).
[287]M. Goldberg, "Viruses and a mathematical problem," J. Mol. Biol. **24**, 337–338 (1967).
[288]S. Torquato, S. Hyun, and A. Donev, "Multifunctional composites: Optimizing microstructures for simultaneous transport of heat and electricity," Phys. Rev. Lett. **89**, 266601 (2002).

[289]R. Zandi, D. Reguera, R. F. Bruinsma, W. M. Gelbart, and J. Rudnick, "Origin of icosahedral symmetry in viruses," Proc. Natl. Acad. Sci. U. S. A. **101**, 15556–15560 (2004).
[290]L. Bowen and C. Radin, "Densest packing of equal spheres in hyperbolic space," Discrete Comput. Geom. **29**, 23–39 (2003).
[291]D. P. Hardin and E. B. Saff, "Discretizing manifolds via minimum energy points," Not. Am. Math. Soc. **51**, 1186–1194 (2004).
[292]O. R. Musin, "The kissing number in four dimensions," Ann. Math. **168**, 1–32 (2008).
[293]V. I. Levenshtein, "On bounds for packings in *n*-dimensional Euclidean space," Sov. Math. Dokl. **20**, 417–421 (1979).
[294]A. M. Odlyzko and N. J. A. Sloane, "New bounds on the number of unit spheres that can touch a unit sphere in n dimensions," J. Comb. Theory Ser. A **26**, 210–214 (1979).
[295]A. B. Hopkins, F. H. Stillinger, and S. Torquato, "Spherical codes, maximal local packing density, and the golden ratio," J. Math. Phys. **51**, 043302 (2010).
[296]A. B. Hopkins, F. H. Stillinger, and S. Torquato, "Densest local sphere-packing diversity: General concepts and application to two dimensions," Phys. Rev. E **81**, 041305 (2010).
[297]A. B. Hopkins, F. H. Stillinger, and S. Torquato, "Densest local sphere-packing diversity: Application to three dimensions," Phys. Rev. E **83**, 011304 (2011).
[298]L. Onsager, "The effects of shape on the interaction of colloidal particles," Ann. N. Y. Acad. Sci. **51**, 627–659 (1949).
[299]D. J. Hoylman, "The densest lattice packing of tetrahedra," Bull. Am. Math. Soc. **76**, 135–137 (1970).
[300]D. Frenkel and J. F. Maguire, "Molecular dynamics study of the dynamical properties of an assembly of infinitely thin hard rods," Mol. Phys. **49**, 503–541 (1983).
[301]A. Bezdek and W. Kuperberg, in *Applied Geometry and Discrete Mathematics: DIMACS Series in Discrete Mathematics and Theoretical Computer Science 4*, edited by P. Gritzmann and B. Sturmfels (American Mathematics Society, Providence, RI, 1991), pp. 71–80.
[302]M. P. Allen, "Simulations using hard particles," Philos. Trans. R. Soc., A **344**, 323–337 (1993).
[303]U. Betke and M. Henk, "Densest lattice packings of 3-polytopes," Comput. Geom. **16**, 157–186 (2000).
[304]S. R. Williams and A. P. Philipse, "Random packings of spheres and spherocylinders simulated by mechanical contraction," Phys. Rev. E **67**, 051301 (2003).
[305]A. Donev, F. H. Stillinger, P. M. Chaikin, and S. Torquato, "Unusually dense crystal ellipsoid packings," Phys. Rev. Lett. **92**, 255506 (2004).
[306]J. S. Bettina and F. A. Escobedo, "Phase behavior of colloidal hard tetragonal parallelepipeds (cuboids): A Monte Carlo simulation study," J. Phys. Chem. B **109**, 23008–23015 (2005).
[307]J. H. Conway and S. Torquato, "Packing, tiling and covering with tetrahedra," Proc. Natl. Acad. Sci. U. S. A. **103**, 10612–10617 (2006).
[308]P. Bolhuis and D. Frenkel, "Tracing the phase boundaries of hard spherocylinders," J. Chem. Phys. **106**, 666–687 (1997).
[309]E. R. Chen, "A dense packing of regular tetrahedra," Discrete Comput. Geom. **40**, 214–240 (2008).
[310]A. Haji-Akbari, M. Engel, A. S. Keys, X. Zheng, R. G. Petschek, P. Palffy-Muhoray, and S. C. Glotzer, "Disordered, quasicrystalline and crystalline phases of densely packed tetrahedra," Nature **462**, 773–777 (2009).
[311]Y. Jiao, F. H. Stillinger, and S. Torquato, "Distinctive features arising in maximally random jammed packings of superballs," Phys. Rev. E **81**, 041304 (2010).
[312]S. Torquato, "Optimal design of heterogeneous materials," Annu. Rev. Mater. Res. **40**, 101–129 (2010).
[313]Y. Kallus, V. Elser, and S. Gravel, "A dense periodic packing of tetrahedra with a small repeating unit," Discrete Comput. Geom. **44**, 245–252 (2010).
[314]E. R. Chen, M. Engel, and S. C. Glotzer, "Dense crystalline dimer packings of regular tetrahedra," Discrete Comput. Geom. **44**, 253 (2010).
[315]A. Jaoshvili, A. Esakia, M. Porrati, and P. M. Chaikin, "Experiments on the random packing of tetrahedral dice," Phys. Rev. Lett. **104**, 185501 (2010).
[316]R. D. Batten, F. H. Stillinger, and S. Torquato, "Phase behavior of colloidal superballs: Shape interpolation from spheres to cubes," Phys. Rev. E **81**, 061105 (2010).
[317]Y. Jiao and S. Torquato, "Communication: A packing of truncated tetrahedra that nearly fills all of space and its melting properties," J. Chem. Phys. **135**, 151101 (2011).
[318]Y. Jiao and S. Torquato, "Maximally random jammed packings of platonic solids: Hyperuniform long-range correlations and isostaticity," Phys. Rev. E **84**, 041309 (2011).
[319]U. Agarwal and F. A. Escobedo, "Mesophase behaviour of polyhedral particles," Nat. Mater. **10**, 230 (2011).
[320]M. Marechal, A. Cuetos, B. Martínez-Haya, and M. Dijkstra, "Phase behavior of hard colloidal platelets using free energy calculations," J. Chem. Phys. **134**, 094501 (2011).
[321]S. Torquato and Y. Jiao, "Organizing principles for dense packings of nonspherical hard particles: Not all shapes are created equal," Phys. Rev. E **86**, 011102 (2012).
[322]J. Henzie, M. Grünwald, A. Widmer-Cooper, P. L. Geissler, and P. Yang, "Self-assembly of uniform polyhedral silver nanocrystals into densest packings and exotic superlattices," Nat. Mater. **11**, 131 (2012).
[323]P. F. Damasceno, M. Engel, and S. C. Glotzer, "Crystalline assemblies and densest packings of a family of truncated tetrahedra and the role of directional entropic forces," ACS Nano **6**, 609–614 (2012).
[324]P. F. Damasceno, M. Engel, and S. C. Glotzer, "Predictive self-assembly of polyhedra into complex structures," Science **337**, 453–457 (2012).
[325]S. Atkinson, Y. Jiao, and S. Torquato, "Maximally dense packings of two-dimensional convex and concave noncircular particles," Phys. Rev. E **86**, 031302 (2012).
[326]R. Ni, A. P. Gantapara, J. de Graaf, R. van Roij, and M. Dijkstra, "Phase diagram of colloidal hard superballs: From cubes via spheres to octahedra," Soft Matter **8**, 8826–8834 (2012).
[327]R. Gabbrielli, Y. Jiao, and S. Torquato, "Families of tessellations of space by elementary polyhedra via retessellations of face-centered-cubic and related tilings," Phys. Rev. E **86**, 041141 (2012).
[328]G. Bautista-Carbajal, A. Moncho-Jordá, and G. Odriozola, "Further details on the phase diagram of hard ellipsoids of revolution," J. Chem. Phys. **138**, 064501 (2013).
[329]A. P. Gantapara, J. de Graaf, R. van Roij, and M. Dijkstra, "Phase diagram and structural diversity of a family of truncated cubes: Degenerate close-packed structures and vacancy-rich states," Phys. Rev. Lett. **111**, 015501 (2013).
[330]R. Gabbrielli, Y. Jiao, and S. Torquato, "Dense periodic packings of tori," Phys. Rev. E **89**, 022133 (2014).
[331]D. Chen, Y. Jiao, and S. Torquato, "Equilibrium phase behavior and maximally random jammed state of truncated tetrahedra," J. Phys. Chem. B **118**, 7981–7992 (2014).
[332]C. Zong, "On the translative packing densities of tetrahedra and cuboctahedra," Adv. Math. **260**, 130–190 (2014).
[333]E. R. Chen, D. Klotsa, M. Engel, P. F. Damasceno, and S. C. Glotzer, "Complexity in surfaces of densest packings for families of polyhedra," Phys. Rev. X **4**, 011024 (2014).
[334]G. Cinacchi and S. Torquato, "Hard convex lens-shaped particles: Densest-known packings and phase behavior," J. Chem. Phys. **143**, 224506 (2015).
[335]M. Dostert, C. Guzmán, F. Mário de Oliveira Filho, and F. Vallentin, "New upper bounds for the density of translative packings of three-dimensional convex bodies with tetrahedral symmetry," Discrete Comput. Geom. **58**, 449–481 (2017).
[336]K. VanderWerf, W. Jin, M. D. Shattuck, and C. S. O'Hern, "Hypostatic jammed packings of frictionless nonspherical particles," Phys. Rev. E **97**, 012909 (2018).
[337]D. Frenkel, B. M. Mulder, and J. P. McTague, "Phase diagram of a system of hard ellipsoids," Phys. Rev. Lett. **52**, 287–290 (1984).
[338]D. Frenkel and B. M. Mulder, "The hard ellipsoid-of-revolution fluid. I. Monte Carlo simulations," Mol. Phys. **55**, 1171–1192 (1985).
[339]D. Frenkel, H. N. W. Lekkerkerker, and A. Stroobants, "Thermodynamic stability of a smectic phase in a system of hard rods," Nature **332**, 822 (1988).
[340]P. J. Camp, C. P. Mason, M. P Allen, A. A. Khare, and D. A. Kofke, "The isotropic–nematic phase transition in uniaxial hard ellipsoid fluids: Coexistence data and the approach to the Onsager limit," J. Chem. Phys. **105**, 2837–2849 (1996).
[341]P. Pfleiderer and T. Schilling, "Simple monoclinic crystal phase in suspensions of hard ellipsoids," Phys. Rev. E **75**, 020402 (2007).
[342]F. Smallenburg, L. Filion, M. Marechal, and M. Dijkstra, "Vacancy-stabilized crystalline order in hard cubes," Proc. Natl. Acad. Sci. U. S. A. **109**, 17886–17890 (2012).
[343]L. Mederos, E. Velasco, and Y. Martínez-Ratón, "Hard-body models of bulk liquid crystals," J. Phys.: Condens. Matter **26**, 463101 (2014).
[344]S. Alexander, "Amorphous solids: Their structure, lattice dynamics and elasticity," Phys. Rep. **296**, 65–236 (1998).

[345]J. N. Roux, "Geometric origin of mechanical properties of granular materials," Phys. Rev. E **61**, 6802–6836 (2000).
[346]C. E. Zachary, Y. Jiao, and S. Torquato, "Hyperuniformity, quasi-long-range correlations, and void-space constraints in maximally random jammed particle packings. II. Anisotropy in particle shape," Phys. Rev. E **83**, 051309 (2011).
[347]S. Torquato and Y. Jiao, "Exact constructions of a family of dense periodic packings of tetrahedra," Phys. Rev. E **81**, 041310 (2010).
[348]J. de Graaf, L. Filion, M. Marechal, R. van Roij, and M. Dijkstra, "Crystal-structure prediction via the floppy-box Monte Carlo algorithm: Method and application to hard (non) convex particles," J. Chem. Phys. **137**, 214101 (2012).
[349]A. Bezdek and W. Kuperberg, "Dense packing of space with various convex solids," *Geometry—Intuitive, Discrete, and Convex* (Springer, 2013), pp. 65–90.
[350]J. de Graaf, R. van Roij, and M. Dijkstra, "Dense regular packings of irregular nonconvex particles," Phys. Rev. Lett. **107**, 155501 (2011).
[351]M. Gardner, *The Colossal Book of Mathematics: Classic Puzzles, Paradoxes, and Problems* (Norton, New York, 2001).